CHALMERS
UNIVERSITY OF TECHNOLOGY

Design of a generic subsystem fixture for physical squeak and rattle prediction

Master's thesis in Applied Mechanics

KHALIL KENAAN
MARKUS YECHOUH

Department of Mechanics and Maritime Sciences
Division of Dynamics
CHALMERS UNIVERSITY OF TECHNOLOGY
Gothenburg, Sweden 2019

MASTER'S THESIS 2019:33

Design of a generic subsystem fixture for physical squeak & rattle prediction

KHALIL KENAAN
MARKUS YECHOUH

Department of Mechanics and Maritime Sciences
Division of Dynamics
CHALMERS UNIVERSITY OF TECHNOLOGY
Gothenburg, Sweden 2019

Design of a generic subsystemfixture for physical squeak & rattle prediction
Khalil Kenaan
Markus Yechouh

Supervisor: Mohsen Bayani Khaknejad, Volvo Cars Corporation
Examiner: Thomas Abrahamsson, Department of Mechanics and Maritime Sciences

Master's Thesis 2019:33
Department of Mechanics and Maritime Sciences
Division of Dynamics
Chalmers University of Technology
SE-412 96 Gothenburg
Telephone +46 31 772 1000

Typeset in LaTeX
Department of Mechanics and Maritime Sciences
Gothenburg, Sweden 2019

Design of a generic subsystem fixture for physical Squeak & Rattle prediction
KHALIL KENAAN
MARKUS YECHOUH
Department of Mechanics and Maritime Sciences
Chalmers University of Technology

Abstract

Today Volvo Car Corporation uses parts of the body-in-white to build a fixture for the instrument panels. However, there is a need for a generic subsystem fixture that can be used instead of the cut-out parts of the body-in-white. The use of a fixture will lower the cost for future testing and decrease the manual work, since the generic fixture will replace a number of cut-out parts from the models. The structure of the generic fixture should thus have some flexibility in geometry, so that it fits a wide range of instrument panel models.

This thesis focus on two vehicle models which will be called model A and B. A benchmark study is performed to get a better understanding of the body-in-whites an particularly in the region where the instrument panels are mounted in the cars. In that, a modal analysis is performed as well as stiffness analysis with the solver Nastran. A meshed solid block is used to allocate the design space of the fixture. The block with the connection parts placed inside are used to perform topology optimisation, where the solid block is the design space and the connection parts is the non-design space. Results from the topology optimisation give guidance on where to place beams and other material when designing the fixture. Using Catia V5 and having the platform drawing of the shaker rig, the design of the fixture was created. The main structural components of the fixture are plates, beams and Aluflex™ components. In Ansa, the model of the fixture is meshed and a modal analysis is performed. Static and dynamic stiffness analysis are also performed, locally and globally, to investigate the stiffness with respect to the body-in-whites.

The main structure of the proposed fixture was shown to have higher global stiffness compared to the body-in-whites. This gives a good foundation for future work. However, local stiffnesses in the connection points are much lower compared to the body-in-whites. This is based on the results from Aluflex, which gives the fixture its generic features. A conclusion from this is that other materials than aluminium profiles needs to be used for parts of the design. Future work could reveal the success of such design strategy. Although steel has a higher density, it can be used in a sophisticated way with other materials to create high rigidity and low weight.

Keywords: generic, fixture, topology optimisation, static and dynamic stiffness, Aluflex™.

Acknowledgements

Our sincere acknowledgement goes to our examiner Prof Thomas Abrahamsson for his support and guidance throughout this thesis work.

We also wish to express our sincere gratitude to our supervisor at Volvo Car Cooperation Mohsen Bayani for his insights and patience. His input have been of great usefulness for us during the project. In addition we would also like to thank our co-supervisors Anneli Rosell and Halil Salifov for the patience and help throughout this project.

Last but not least we would like to thank the entire solidity team at Volvo Car Cooperation for their invaluable help during our thesis work, especially Henrik Viktorsson and Henrik Puhasmägi.

Khalil Kenaan, Markus Yechouh, Gothenburg, June 2019

Nomenclature

Abbreviations

A	Amplitude	
BIW	Body in White	
CAD	Computer-Aided Design	
CAE	Computer-Aided Engineering	
FE	Finite Element	
FEM	Finite Element Method	
FFT	Fast Fourier Transform	
IP	Instrument Panel	
KSK	Climate shaker rig	
maxdim	Maximum dimension	
mindim	Minimum dimension	
S&R	Squeak and Rattle	
SOL103	Nastran solver 103	
SOL111	Nastran solver 111	
SUV	Sport Utility Vehicle	
VCC	Volvo Car Corporation	
Physics Constants		
$\ddot{\boldsymbol{u}}$	Acceleration	m/s^2
$\dot{\boldsymbol{u}}$	Velocity	m/s
$\boldsymbol{\omega}$	Eigenvalue	rad/s
$\boldsymbol{C}$	Damping matrix	
$\boldsymbol{K}$	Stiffness matrix	N/m
$\boldsymbol{M}$	Mass matrix	kg
$\boldsymbol{U}$	Eigenvector	
$\boldsymbol{u}$	Displacement	m

Contents

List of Figures

1
Introduction

In this chapter the introduction of the project is presented. Initially the background of the problem is presented followed up by the objective, aim and limitations.

1.1 Background

The solidity group at Volvo Car Cooperation (VCC) are, among other things, responsible for the handling of Squeak and Rattle sounds (S&R) and the solid feeling in the car. S&R are non-stationary sounds that occur when two parts come in contact with each other, either by direct impact or by sliding motion. The absence of perceivable S&R is a must for premium cars. Part of VCC's main scope is setting requirements and verification of S&R problems in early design phases and not after production launch. One of the major challenges is to improve the competence for attribute verification to meet shorter lead time. To reduced the number of physical complete vehicle prototypes, the company uses a subsystem level test rigs.

One main issue is having a well-constructed fixture to mount the Instrument Panel (IP) for subsystem testing. Applying the proper boundary conditions on the subsystem and securing the system response are here some of the challenges. Previously, VCC have been constructing a fixture from parts of the Body-in-White (BIW) to perform tests in the shaker rig to examine IPs as subsystems. This is costly since each IP model needs a cut-out fixture from the corresponding BIW.

1.2 Objective

The objective of this thesis work is to design a generic fixture that can be used for different IPs for the purpose of S&R-evaluation in the shaker rig. Since the fixture should be generic, there will be some adjustable mechanisms to vary some parameters to fit different IPs. The aim is thus to replace the cut-out parts from the BIW with a fixture that have following points checked out:

- A designed fixture which is manufacturable
- Generic features that can be manually adjusted locally
- Higher global stiffness compared to the area where the IPs are mounted in BIWs
- Higher local stiffness in the connection points compared to the BIWs

1.3 Limitations

There were some limitations in this thesis project that has to be taking into account. One important limitation is the amount of time. The work is limited to what two students working approximately 40 hours per week for 20 week can accomplish. The FE-model for the IPs and the BIWs is provided by VCC. For that reason a mesh convergence study for the IPs and BIWs was not a part of this project. Another limitation in this project is that only linear approximated simulations will be performed. For that reason the Nastran solver can be employed to the advantage. Finally, no physical prototype of the fixture will be build because of the time limitations in this project. The adjustable mechanism will include variation in positions, but no stiffness adjustment.

This thesis work concerns two car models further referred to as model A and model B. This is because these cars utilise two different platforms. The final fixture together with an IP cannot weigh more than 150 kg in total because of the limitation of the shaker rig.

2
Theory

This chapter briefly describes the theory behind modal analysis, stiffness and topology optimisation.

2.1 Squeak and Rattle mechanism

Squeak is a sound which is induced by friction from two surfaces in contact and sliding in the opposite direction against each other [1]. To generate squeak there must be a relative motion between the two surfaces. Not all relative motion produce squeak. One of the fundamental squeak generation mechanisms is unstable vibration that has stick-slip motion characteristics. The occurrence of stick-slip may depend on loading condition such as contact pressure, sliding speed, surface profiles, material properties, and most importantly the characteristics of the coefficient of friction. However, the properties of the material may also be affected by temperature and humidity.

Rattle is described as "an impact-induced phenomenon that occurs when there is a relative motion between components with a short established of contact"[2]. Rattle usually occurs from loose or flexible components in the structure. Due to insufficient attachment the flexible components will repeatedly separate and be in renewed contact causing the rattle sounds [2].

2.2 Verification

A model verification is described as a process of evaluating systems to determine whether the products of a given development phase satisfy the conditions imposed at the start of that phase [3]. Verification is with other words a test that is done to prove that the specified requirements for a system are met during the development.

2.3 Modal analysis

The study of basic dynamic properties of systems is called modal analysis [4]. The basis of modal analysis is the modes of vibration that occurs naturally if the system is excited by an impact. A modal analysis describes the deformation of the system, each natural frequency corresponds to a natural mode. The fundamental properties of a structure is dependent on the material stiffness, mass and damping. This will determine structural vibration behaviours when the structure is exposed to operational loads [5]. The natural modes and natural frequencies are computed by solving the the non-trivial solution for the equation of motion [6]. A dynamic system with damping can be described with the following equation of motion:

$$\boldsymbol{M}\ddot{\boldsymbol{u}}(t) + \boldsymbol{C}\ddot{\boldsymbol{u}}(t) + \boldsymbol{K}\boldsymbol{u}(t) = \boldsymbol{p}(t) \tag{2.1}$$

with $\boldsymbol{M}, \boldsymbol{C}$ and $\boldsymbol{K}$ denoting the mass, damping and stiffness matrix respectively. The displacement, velocity and acceleration of the system are $\boldsymbol{u}, \dot{\boldsymbol{u}}$ and $\ddot{\boldsymbol{u}}$. Lastly the loads are represented as $\mathbf{p}$.

The free vibration equation of motion is obtained when the force and the damping in equation 2.1 is set to zero. The equation of motion for the free vibration will then be:

$$\boldsymbol{M}\ddot{\boldsymbol{u}}(t) + \boldsymbol{K}\boldsymbol{u}(t) = 0 \tag{2.2}$$

It is assumed that the harmonic motion is:

$$\boldsymbol{u}(t) = \boldsymbol{U}cos(\omega t - \alpha) \tag{2.3}$$

When inserting the harmonic motion into the equation of motion for the free vibration (2.2) the following equation is obtained:

$$[\boldsymbol{K} - \omega^2\boldsymbol{M}]\boldsymbol{U} = \mathbf{0} \tag{2.4}$$

By solving the equation the eigenvalues ω and the eigenvectors $\boldsymbol{U}$ are obtained.

2.4 Stiffness

Stiffness is defined by the displacement in an object that occurs when applying a specific force [7]. The more rigid the structure is the higher the stiffness will be. The stiffness of a structure can be a constant or be dependent on the loading of the system.

2.4.1 Calculations

Finite element modelling techniques are used to establish the model given by equation 2.1. The global stiffness matrix $\boldsymbol{K}$ in equation 2.1 is achieved by assembling the element stiffness matrices. The element stiffness matrix of the linear elastic material is given as

$$\boldsymbol{K}^e = \int_{V^e} \boldsymbol{B}^T\boldsymbol{D}\boldsymbol{B}dV^e \tag{2.5}$$

where $\boldsymbol{D}$ is the material stiffness matrix and $\boldsymbol{B}$ is the strain-displacement matrix [8].

2.4.2 Static stiffness

Static stiffness is the inverse of the ratio of how much an object deflects for an applied force [9]. If the object is very flexible, this means that is has low static stiffness and vice verse, a less flexible object has higher static stiffness.

To obtain the static stiffness of a body, the static force is divided by the deflection of a certain point where the force is applied.

$$k_s = \frac{F}{d} \tag{2.6}$$

Another way to obtain the static stiffness is from the dynamic stiffness (see next section). From the dynamic stiffness function the stiffness at 0 Hz constitutes the static stiffness [10].

$$k_s = k_d(0) \tag{2.7}$$

2.4.3 Dynamic stiffness

While a car is driving, the road excites the BIW with a time-varying load that can be decomposed to loads associated with specific frequencies. The stiffness of the body varies with the frequency of the loading. According to Piersol [9], the dynamic stiffness is the ratio of the change of force to the change of displacement under dynamic conditions. The dynamic stiffness of the BIW is thus important to take into account for the designing of the fixture. The local dynamic stiffness can be written as a function of the frequency:

$$k_d(f) = \frac{F(f)}{d(f)} \tag{2.8}$$

where F is the force, d is the displacement and f is the frequency of the excitation.

2.5 Topology optimisation

Topology optimisation is a mathematical method used to optimise a certain body within a given design space, i.e. for best distribution of material for the optimisation goal and some constraints. Within the design space it is possible to obtain any design. The Finite element method (FEM) is used to assess the design performance and gradient based mathematics are used to solve the optimization problem [11]. The optimisation problem can be stated as [12]:

$$\begin{aligned} &\text{Minimise} \quad f(\boldsymbol{\rho}) \\ &\text{Subject to} \quad g_j(\boldsymbol{\rho}) - g_j^U \leq 0, \quad j = 1, ..., M \\ &\qquad\qquad\qquad 0 \leq \rho_i \leq 1, \quad i = 1, ..., N \end{aligned} \tag{2.9}$$

where $f(\boldsymbol{\rho})$ is a representation of the objective function, $g_j(\boldsymbol{\rho})$ and g_j^U represents the j-th constraint respond and its upper bound, respectively. M is the number of constraints; ρ_i is the normalised material density of the i-th element constrained to stay within range of 0 to 1. Topology optimization is a very powerful and useful tool for early stage of the design. However, the suggested design by topology optimisation are not always practically achievable for a specific manufacturing process.

2.5.1 Optistruct

The solver Optistruct for topology optimisation solves the problem by using the local approximation method, which is an iterative procedure [13]. The solution of the optimisation problem is determined by five steps in an iterative procedure, Figure 2.1. Firstly, analysing the problem using finite elements, then a convergence test to see whether the design has converged or not, followed by a response screening performed to retain potentially active responses for the current iteration. A design sensitivity analysis is than carried out for retained responses and lastly, using the sensitivity information, the optimisation of the explicit approximated problem is performed, before turning back to re-analyse the problem. The design variables change during each iteration to achieve the optimum solution. However, the largest design variable changes occur in the first few iterations.

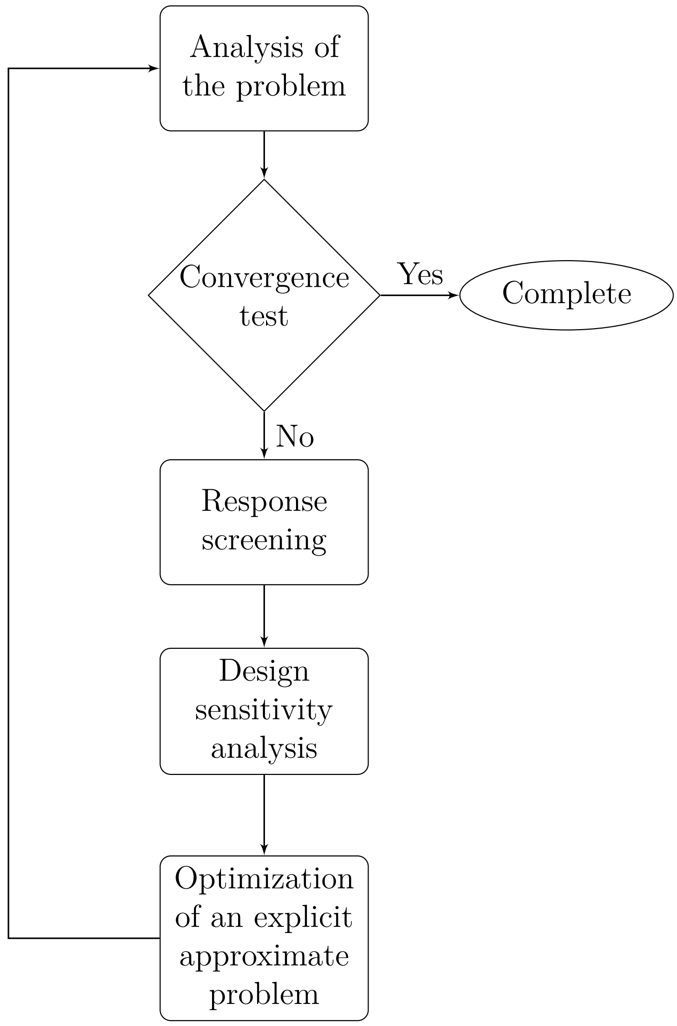

Figure 2.1: Flow chart of the method of the optimisation problem.

3
Method

The methodology used can be summed up in five major areas: benchmark study, testing of the existing fixtures, topology optimisation, designing of a generic fixture and lastly verification of the final fixture design. This is illustrated in the flow chart in Figure 3.1. The pre- and post-processor programs Ansa and Meta were used for the benchmark study, with Nastran as solver. Regarding topology optimisation, Hypermesh and Hyperview were used as pre- and post-processors with Optistruct as the solver.

3.1 Benchmark study

A benchmark study with modal analysis and stiffness analysis was conducted of the IPs and BIWs for the two Sport utility vehicle (SUV) models A and B. These models are based on two different platforms. This variation of models is a good base for designing a generic fixture. Since the fixture should behave similar to the respective BIWs it was critical to investigate the modal behaviour and stiffness (static and dynamic) of the structures. The FE-models of the IPs and BIWs for the two models were prepared. However, very little preparation of the IP and BIW models was needed, because well meshed FE-models were provided to us.

3.1.1 Modal analysis

Modal analysis was performed to capture the natural frequencies of the system assembly. The modal analysis was performed on the IPs as well as the BIWs for the models A and B. The Nastran solver 103 (SOL103) was used to compute the first 50 eigenmodes, since the more fundamental global behaviour is well captured for eigenfrequencies below 50 Hz.

Figure 3.1: Flow chart of the methodology of the project.

3.1.1.1 Boundary conditions

To investigate the natural frequency of the IPs and BIWs boundary conditions were applied on the models. The modal analysis was performed separately for the IPs and the BIWs. Two different boundary conditions cases were set on the IPs to investigate how the different placed boundaries influenced the models. In the first case, the models were free in space, which means that all system boundaries were free. The second case was when the IP models were clamped at the connection points, this can be seen in Figure 3.2 for model B and in Figure 3.3 for model A. In the case of the BIWs, the boundary conditions was set to be clamped at the sub mounts points when performing the modal analysis.

3.1.2 Stiffness Analysis

The stiffness analysis comprise of static and dynamic stiffness, which were computed only on the BIWs of model A and B. The generic fixtures main aim is to reflect higher local and global stiffness from the BIWs on to the IPs.

3.1.2.1 Connection points

The stiffness analysis was performed in the connection points on BIWs, where the BIWs are connected to the IPs. The number of connection points between the BIWs and IPs differs for the two models. Model B have totally 12 connection points, 8 main connection points and 4 clips seen in Figure 3.4. Model A have 14 connection points consisting of 9 main connection points and 5 clips which can be seen in Figure 3.5.

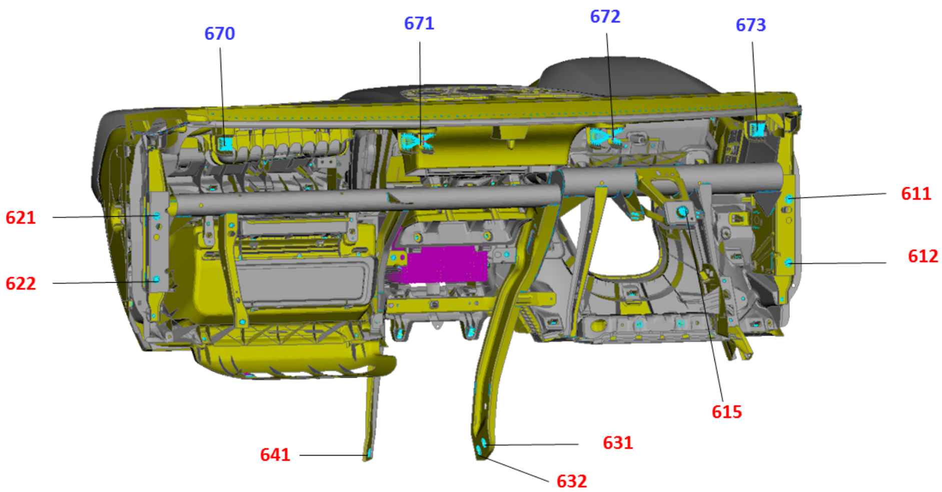

Figure 3.2: Connection points between the IP and BIW for model B, with node IDs highlighted.

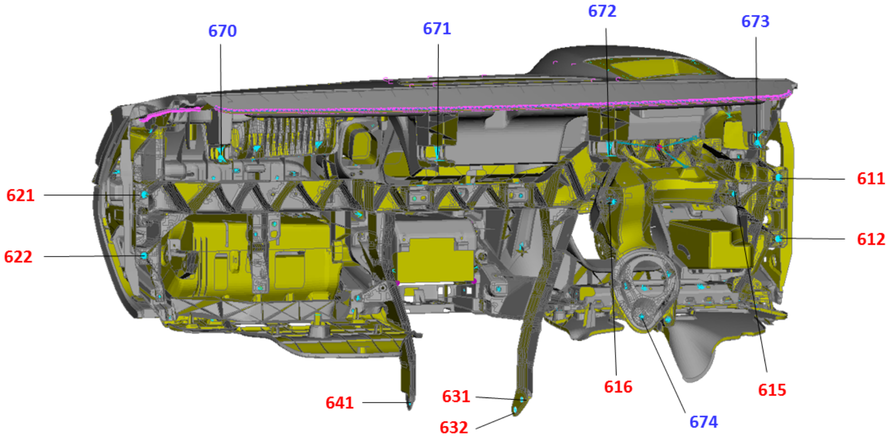

Figure 3.3: Connection points between the IP and BIW for model A, with node IDs highlighted.

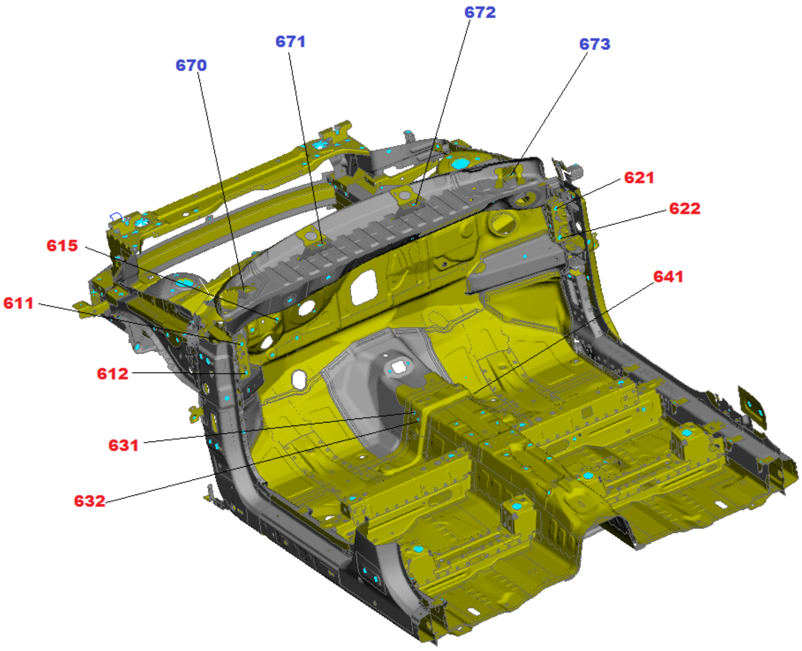

Figure 3.4: Connection points between the IP and BIW for model B, with node IDs highlighted.

3.1.2.2 Boundary conditions

To analyse the models, boundary conditions were applied. Three different boundary conditions cases were set on the BIWs to investigate the influence on stiffness. The boundary condition placements are highlighted with white points and can be seen in Figure 3.6 for the model B and Figure 3.7 for the model A. The first boundary

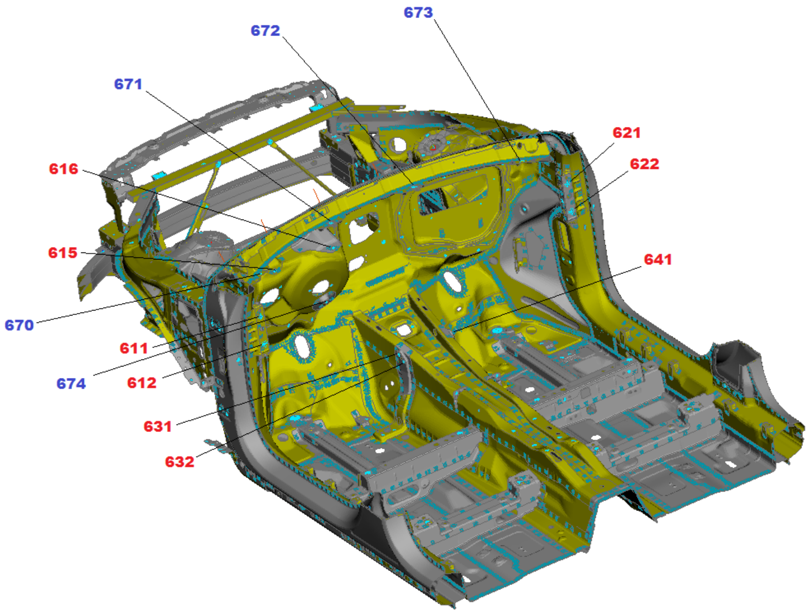

Figure 3.5: Connection points between the IP and BIW for model A, with node IDs highlighted.

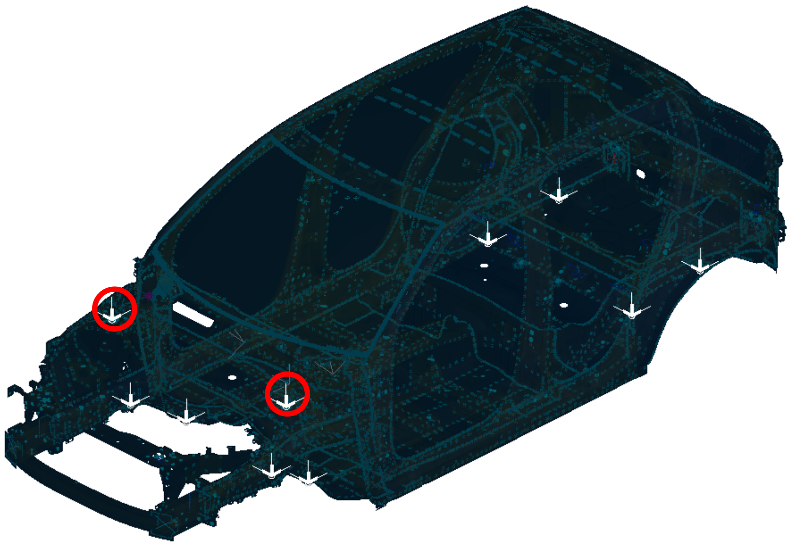

Figure 3.6: The model B BIW boundary condition with the top mounts highlighted.

condition case was when the BIWs were free in space. The second case was when the BIWs were clamped at the sub mounts. The third case was when the BIWs were clamped at both the sub mounts and top mounts, where the top mounts are highlighted with red circles.

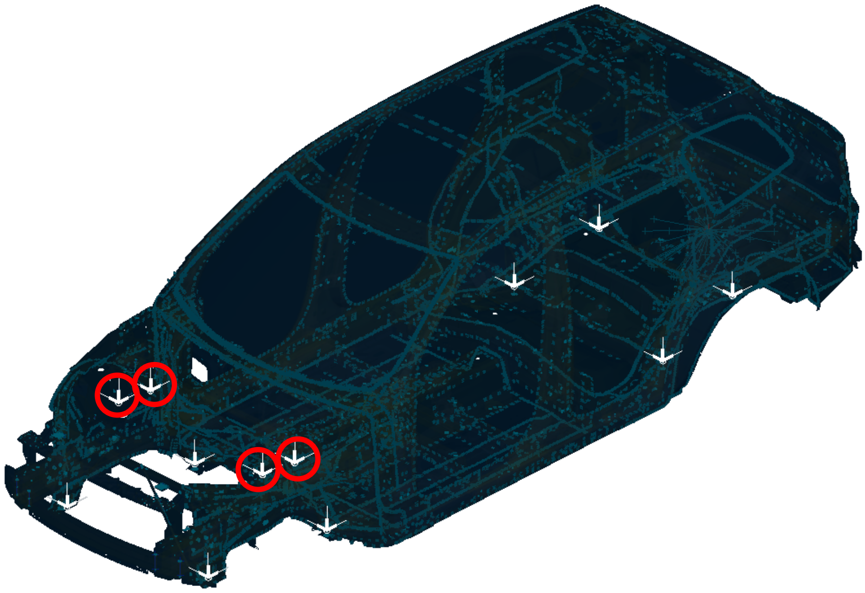

Figure 3.7: The model A BIW boundary condition with the top mounts highlighted.

3.1.3 Static and dynamic stiffness

Static stiffness for the BIWs were calculated in the main connections points which are highlighted in Figures 3.4 and 3.5. Using Nastran solver SOL111, they were calculated for the three different boundary condition cases mentioned. Dynamic stiffnesses are also calculated in the connection points of the BIWs, with the same solver. It computes the point mobility in the selected connection points which gives the dynamic stiffness. With dynamic stiffness, the variation of stiffness for different frequencies is received. The most interesting result is the dynamic stiffness in the frequency range of $0 - 100$ Hz, because that is where the modes that involves a more overall (global) motion can be found.

3.1.3.1 Global stiffness

The global stiffnesses of the BIWs are important parameters when designing a fixture. In order to capture the global stiffness values the BIWs were rigidized between the A-pillars and the A-pillar brackets with rigid links, which can be seen in Figures 3.8(a) and 3.8(b). The static and the dynamic stiffness of the global structure were calculated in the master node of the rigidisation, highlighted in the figure with a red circle.

3.2 Testing in the shaker rig

To be able to validate the result from a future generic fixture for the IPs, vibration testing of already existing fixtures were conducted with the IPs mounted for model A and B. The used fixtures consist of cut-out parts from the BIWs. Existing fixtures

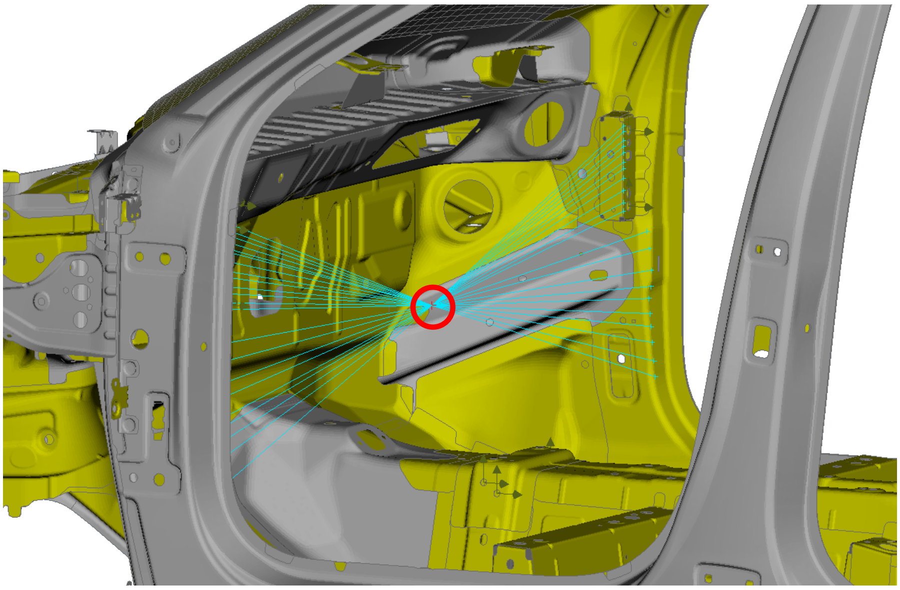

(a) The rigidisation of model B BIW with highlighted master node.

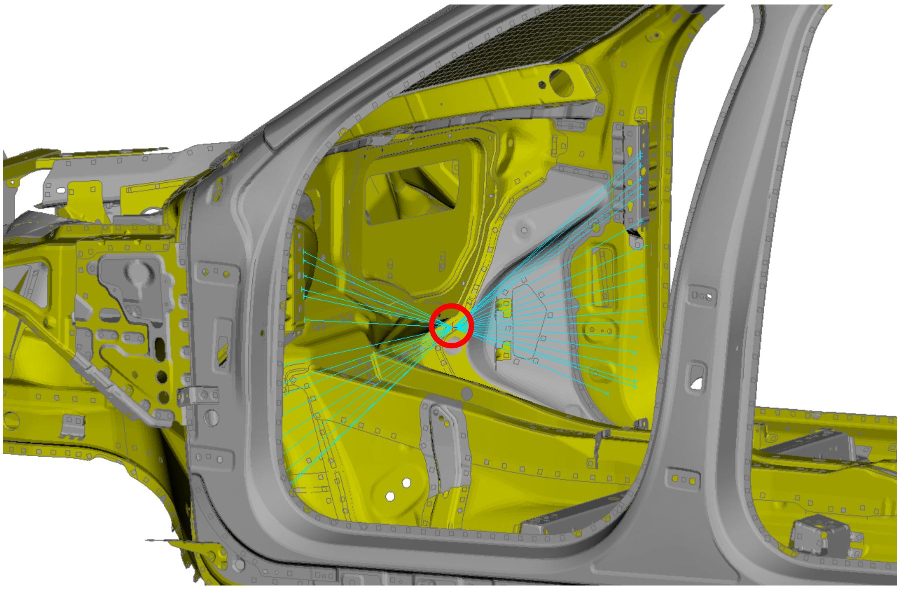

(b) The rigidisation of model A BIW with highlighted master node.

Figure 3.8: The rigidisation of the BIWs with the master node highlighted in red.

for the models were used to mount the IPs to the shaker rig. The testing was performed for different roads signals, sine sweeps and sensor placements.

3.2.1 Excitation signals

Two kinds of signals were used for exciting the shaker rig system during the testing: road signals and sine sweeps.

3.2.1.1 Road signals

The road signals used for the testing on both model A and B were output responses of the climate shaker rig (KSK) test for model B. The KSK signals were provided from VCC. Six different road signals were used for the testing, where all of the road signals have been obtained from physical testing on real roads. The signals used on the shaker rig are:

- Road case 1 with speed 40 km/h to 70 km/h
- Road case 1 with speed 60 km/h
- Road case 2 with speed 25 km/h
- Road case 3 with speed 20 km/h to 40 km/h
- Road case 3 with speed 30 km/h
- Road case 4 with speed 60 km/h

The first road case is an uneven country road scanned in the United Kingdom. Road case 1 was tested for different speeds. Firstly, when the car was driving with a constant speed of 60 km/h and secondly when the car was accelerating from 40 km/h to 70 km/h. Road case 2, which is the roughest road used, is a road made of large paving stone, the road was measured for the speed of 25 km/h. The third road case is similar to the second road case, however, the paving stones are smaller and more smooth. Like road case 1, the third case was tested for different speeds, a constant speed of 30 km/h and an accelerating speed of 20 km/h to 40 km/h. Lastly road case 4 is similar to the first case, with the difference being the road is coarser and have bigger disturbances. The last road case was measured for the speed of 60 km/h.

3.2.1.2 Sine sweep signals

A sine sweep is a sine function with frequency that vary over time. Two different cases of sine sweep were used for the testing: in-phase sine sweep and out-of-phase sine sweep. An in-phase excitation is formed when the system excitation the left and right sides are in phase.
The goal was to construct sine sweeps that go from high to low amplitudes while increasing the frequency, which results in that a constant input power is supplied to the system. The in-phase sine sweep was manually constructed from the following sine function:

$$y = A(f)sin(2\pi ft) \tag{3.1}$$

Two different sine sweeps were constructed for the in-phase case. The reason for this was mainly to investigate how the amplitude would affect the testing result. The difference between the two cases was the amplitude A. The functional form of the amplitudes used for the two cases were:

$$A(f) = \frac{A_0}{f} \quad \text{and} \quad A(f) = \frac{A_0}{f^2} \tag{3.2}$$

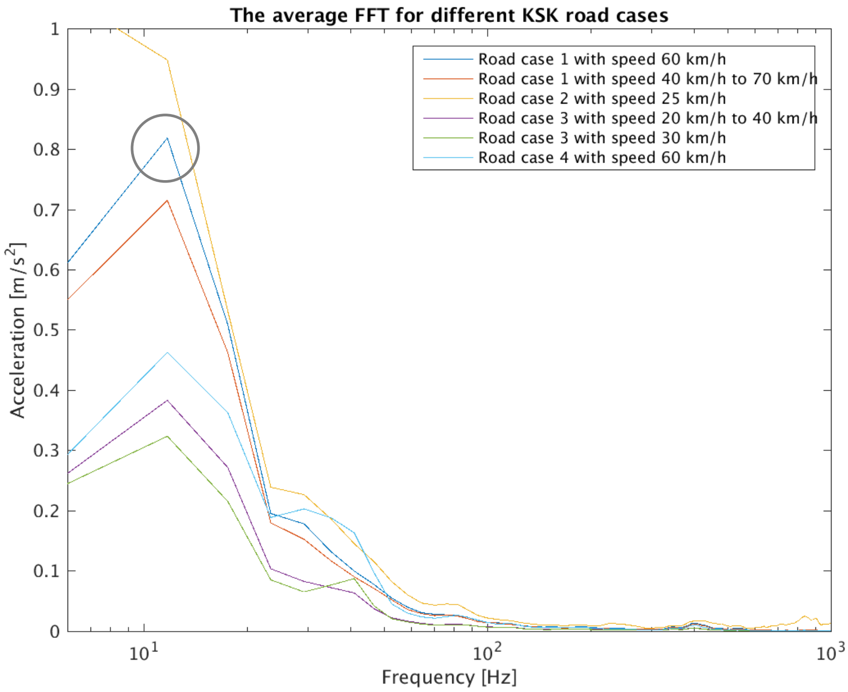

Figure 3.9: The average FFT plot for different KSK road cases with the used peak highlighted.

where the constant A_0 was obtained by examining the average Fast Fourier transform (FFT) in Figure 3.9 for the KSK road cases. The average FFT for the different KSK road cases were measured at the right A-pillar in the local z-direction. The constant maximum amplitude A_0 was obtained by multiplying the acceleration with the respective frequency at one of the highest peaks, highlighted in Figure 3.9.

3.2.2 Accelerometer placements on the IP for model B

Accelerometer placements for model B were chosen according to several critical areas where S&R occurs. The accelerometers used for the tests are multi-axis models to measure the acceleration in three axis (x,y and z-direction). To check the quality of the excitation signals, two sensors were placed on the upper right and upper left A-pillar connection point. The measured signals in these points were later compared to the excitation signals in order to see if the measured signals are reliable.

3.2.3 Accelerometer placements on the IP for model A

Accelerometers for the A model were placed on similar locations as for the model B. The choices were again based on several critical areas where S&R is generated. However, due to some differences in geometry between the two models some changes in accelerometer placement were made. Also here, accelerometers were placed on the upper right and upper left A-pillar connection point in order to later compare the measured signals with the excitation signals as a quality check.

3.3 Pre-design phase

In the pre-design phase of the generic fixture, a topology optimisation was performed based on stiffness data from the benchmark study. The results from the topology optimisation was then used as an indication of material distribution to be used for a more detailed fixture design.

3.3.1 Model

Since there was no existing design to work from, the simplest way to start was to begin with a solid block of material, excluding the volume were the IP and the tunnel needed room. The volume of the solid block of material was based on model A, the reason for this was because it was the larger of the two models. In Ansa, the solid block was created with the dimensions 2200 mm × 2000 mm × 1050 mm with 1.7 million solid elements, where 1.26 million elements were hexahedron, 470 000 elements were tetrahedron elements and 15 000 were pentahedron elements. The connection parts of the BIW from model A were included in the solid as connection for the IPs, and to which to apply forces. They are kept seperate from the design space, meaning that they will not be affected by the topology optimization process. The shaker rigs platform was also imprinted under the solid box as seen in Figure 3.10(a).

3.3.2 Topology optimisation

The software used for topology optimisation was HyperWorks, which is a complete CAE software made by Altair Engineering that has a universal finite element solver as well as pre- and postprocessors. The HyperWorks structural analysis solver Optistruct, which is a solver used for design and optimizing, was used for the optimisation problem. Hypermesh and Hyperview were used for pre- and post-processing.

The solid block was imported to HyperMesh, where the design space, boundary condition and forces were defined. The boundary conditions were set on the bottom of the solid block, more specifically, where the fixture will be mounted on the shaker rig, which can be seen in Figure 3.11.

3.3.2.1 Objective and constraints

Results from the static stiffness analysis in the benchmark study were used during the topology optimisation. This was executed by inverting the static stiffness values to obtain the x, y and z displacement of eleven reference nodes. Forces of 1 N is also placed in each node. For each load step, an optimal response and an optimal constraint was created with displacement as constraint. Another constraint was created for the volume fraction, where the specific fraction that should be left after the optimisation was specified.

A topology optimisation to minimise the free volume to find the best distribution of material and satisfying the set of constraints of the displacement and volume fraction was tried. However, as obvious from inspection this approach did not result

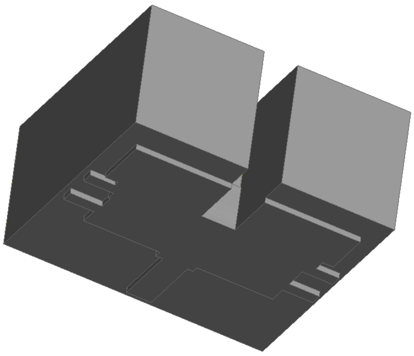

(a) Bottom view of the block of material.

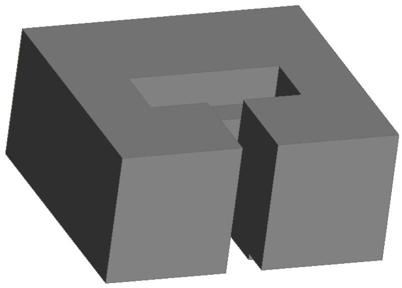

(b) Top view of the block of material.

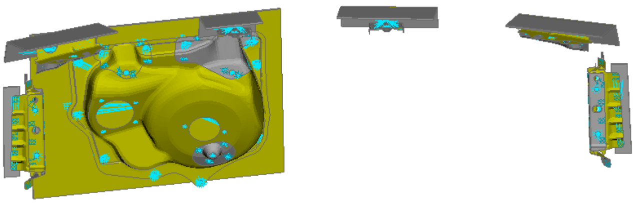

(c) Connection part inside the block of material.

Figure 3.10: Block of material and connection part used for the topology optimisation.

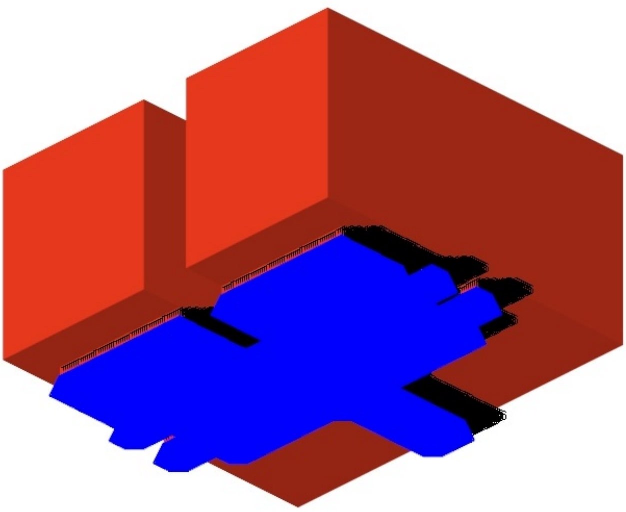

Figure 3.11: The boundary condition set on the solid box.

in feasible result, on which fixture design could be based. For that reason a different approach was chosen. The weighted 33 compliances was chosen as the scalar objective in the minimisation of the volume to find the best distribution of material. A volume fraction was chosen as an optimisation constraint to leave 25% of the available material.

To avoid having unconnected materials free in space the function minidens was used. The function mindens aims to minimise the density meaning that density lower than a determined value would be removed. To be able to obtain a design with a beam-like structure two new function were added: mindim (minimum dimension) and maxdim (maximum dimension). By inserting a maximum dimension of 20 mm and a minimum dimension of 2 mm, the materials merged into a beam-like structure with cross-section dimensions between 2 mm and 20 mm.

3.4 Fixture Design

The next step in the methodology was to use the knowledge and data gained from the benchmark study and the result from topology optimisation to design the generic fixture. In the design, an adjustable mechanism for the fixture was included. The CAD software Catia V5 was used during the designing process.

3.4.1 The design

The design of the fixture was created by using the results from the topology optimisation as guidelines, since they gave an idea of where to place material when designing the fixture. Three major considerations were found important in designing the fixture. Firstly, how the beams should be placed and how parts of the fixture should be connected. Secondly, the weight of the fixture had to be taken into account, because a limitation of the shaker rig was 150 kg and an IP itself weighs approximately 60 kg. By having a safety margin of 20 kg, the fixture weight was set to be around 70 kg. Lastly, manufacturability also had to be taken into account when designing the fixture. By using existing components and cross sections on beams the complexity of the design and manufacturability was decreased.

Data from shaker rig and the result from the topology optimisation were used in, the design of the fixture. The process of designing the fixture was iterative. A preliminary design of the fixture was made. However, when examining both the eigenmodes and strain energy of the structure some potential areas of improvement were found. Additional beams were added at those critical areas for the proposed design of the fixture, which can be seen in the result chapter.

3.4.1.1 Adjustable mechanism

Since the objective was to make the fixture generic, a mechanism for adjusting the connection points locally on the fixture had to be created. The generic mechanism can be divided into three major areas: the main A-pillar brackets, the centre connections and the clips. The localisation of A-pillar brackets for the two models A and B differs. A mechanism for these brackets was constructed be able to change position of connection points. The adjustable mechanism for the centre connection was designed similarly, in order to fit both models. Lastly, the clips connections were designed so that they could be moved with the same mechanism used for the A-pillar brackets and centre connections. However, the clips connection from the BIWs for the respective model were used on the fixture for the mounting of the IP, since they have heavily specialised designs.

3.5 Verification

To be able to compare the results of the BIW to the fixture, a verification study was finally performed. The verification of the fixture was executed by studying the stiffness properties of the fixture and the modal behaviour. The static and dynamic stiffness behaviour of the designed fixture was compared with the static and dynamic behaviour of the BIW for model A.

3.5.1 Model

To do verification on the fixture, the pre-processor software Ansa was used. FE shell elements that represent the middle skin of the solids were created, i.e. the mid surfaces were extracted and some simplifications were done. The surfaces were meshed with 120 000 quad shell elements as can be seen in Figure 3.12. By using rigid links (RBE2 elements) different part of the fixture, bolts and welding were connected.

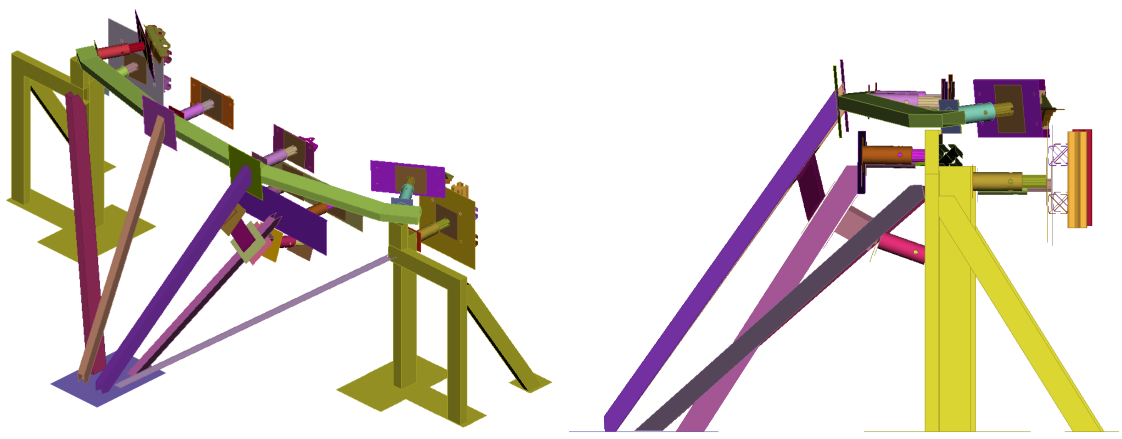

(a) Isometric view of the meshed fixture. (b) Top view of the block of material.

Figure 3.12: Meshed mid surfaces of the fixture.

3.5.2 Static and dynamic stiffness

The next step was to compute the static and dynamic stiffness of the designed fixture. The local and global static and dynamic stiffness were calculated. The local stiffness of the fixture was calculated in both the main connection points and the clips. Since the topology optimisation was based on model A, the local static and dynamic stiffness of that BIW was compared to the final fixture. The connection points on the fixture were therefore set to be in the same position as for model A. Boundary conditions on the fixture were set to be clamped on the bottom plates, highlighted in Figure 3.13, which are screwed to the shaker rig platform. The connection points between the IP and the fixture can be seen in Figure 3.13. The global static and dynamic stiffness were also calculated for the fixture, in a similar way to the BIWs. The fixture was rigidized in between the A-pillar and A-pillar brackets as shown in Figure 3.14, whereas the static and dynamic stiffness were calculated in the highlighted master node of the rigidisation.

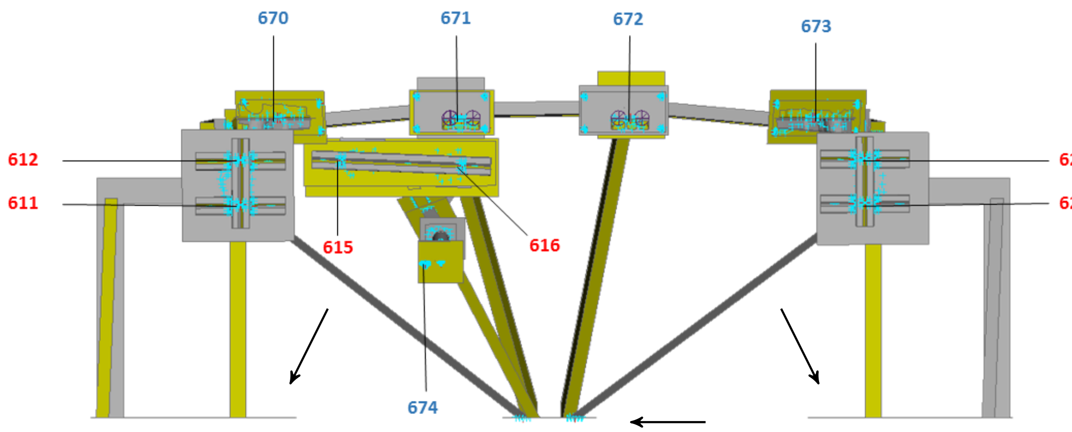

Figure 3.13: Connection points between the fixture and the IP of model A with highlighted bottom plates.

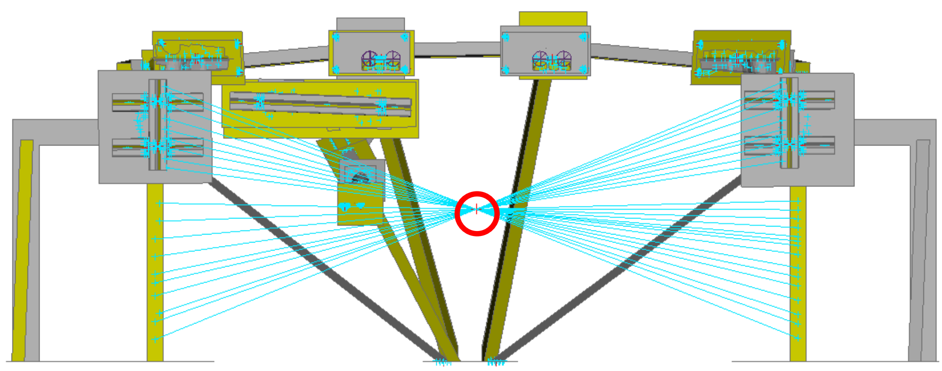

Figure 3.14: The rigidization of the fixture with highlighted master node.

4
Results and Discussion

The results of the benchmark study, testing, topology optimisation, design of the fixture and lastly verification of the fixture are presented in this chapter.

4.1 Static stiffness

Static stiffness result of the BIWs for models A and B are presented in Figure 4.1. The bar plots shows static stiffness in the connection points of the BIWs. Static stiffness are computed for three different boundary conditions on the BIWs. Overall, the stiffness varies between different connection points and different boundary condition. Some of the boundary conditions are higher for A and some are higher for B.

By examining the stiffness results, one boundary condition case is chosen for the design of the generic fixture. Since the static stiffness plots, shown in Figure 4.1, have small differences for the different boundary conditions, the second boundary condition case where the BIWs were clamped at the sub mounts, is chosen for the design of the fixture. Main reason for that is because this case reflect the reality of where the car is fixed.

4.1.1 Dynamic stiffness

The dynamic stiffness was computed for the BIWs of model A and B in the main connection points. The results can be seen in Appendix A. The overall stiffness of model A is higher compared to model B which is reasonable since model A is the larger of the two.

4.2 Testing

4.2.1 Sine sweep signals

The two in-phase sine sweep cases can be seen in Appendix B.1 and B.2 with the respective Fast Fourier Transform for each case. Both cases have high amplitudes in the beginning but gradually decreases with an increasing frequency. It can be seen in the FFT figures that the amplitudes decrease for larger frequencies. This results in a constant energy input to the system.

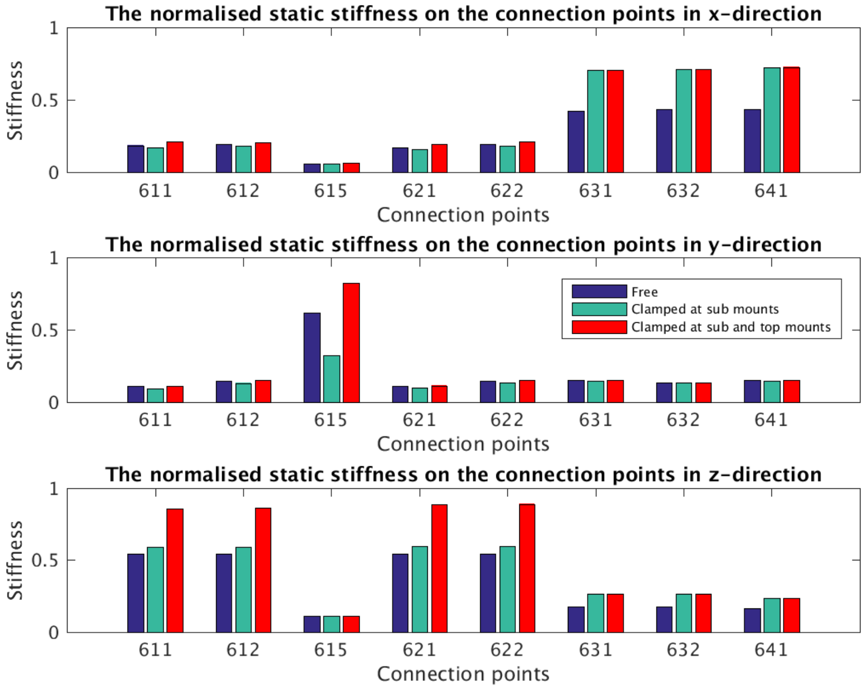

(a) The normalised static stiffness in the connection points for model B.

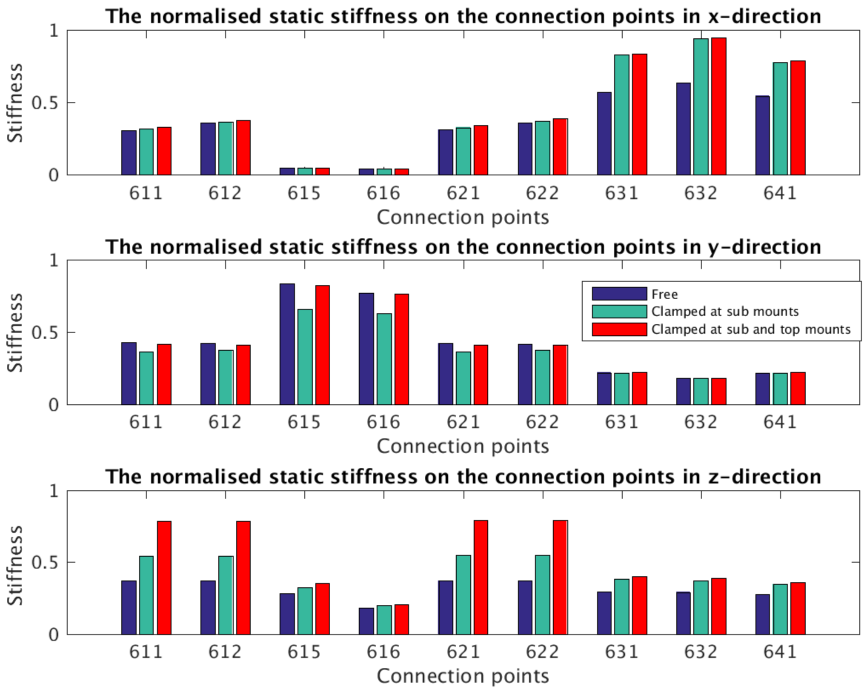

(b) The normalised static stiffness in the connection points for model A.

Figure 4.1: The normalised static stiffnesses.

4.2.2 Quality Check

A quality check of the testing is performed by comparing FFT of the excitation signals, which excites the system, with FFT of measured signals on the right upper A-pillars. The six signals, which were measured for the two models, are used for quality check. Quality check for the two models are shown in Appendix B.4 and B.3.

4.3 Pre-design phase

The topology optimisation result is used as a guideline for design of the fixture.

4.3.1 Topology optimisation

The topology optimisation converged and gave a feasible design according to Hyperworks default criteria. In Figure 4.2(a) and 4.2(b) the topology optimisation results are shown together with an indication of the initial solid block and in Figure 4.2(c) the connection parts are also visible inside the volume. The suggested design gives a rough estimate on where material should be placed to fulfil the criteria that have been set. Approximately 60% of material from the initial solid box is removed.

As seen in Figure 4.2, the bulk of the material that remains are concentrated around the connection parts. This is expected since forces for the topology optimisation were applied in the connection points. Another interesting result is how material have been placed in the highlighted parts in Figure 4.2(a) and 4.2(b). The topology optimiser hinted on keeping materials in rear part of the block highlighted in Figure 4.2(a). Presumably, material is left there to better stabilise the structure and to increase stiffness. The next interesting material placement is highlighted in Figure 4.2(b), where the topology optimisation kept material to form some kind of casing. This is again probably to stabilise the structure which results in a stiffer structure.

4.4 Fixture Design

In this section results of the fixture design is presented.

4.4.1 Primary design

The fixture is mainly constructed using beams, plates and Aluflex™ profiles, which can be seen in Figure 4.3. Aluflex™ is a company that makes a variety of aluminium components commercially used in the industry. This design and placement of the components are based on the topology optimisation. The weight of the fixture is 63 kg which gives a 7 kg of margin for screws and bolts. Profiles and material used for the fixture are common and frequently used, thus minimising complexity for future manufacturing.

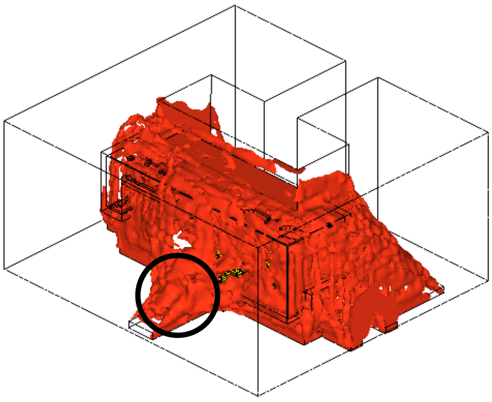

(a) Isometric view of the topology optimisation with the solid box and interesting material placements highlighted.

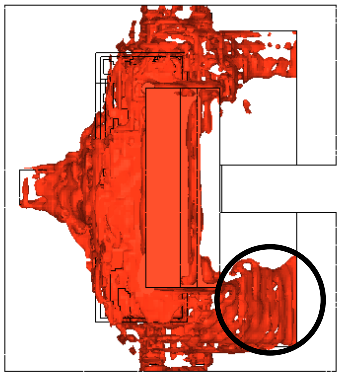

(b) Top view of the topology optimisation with the solid box and interesting material placements highlighted.

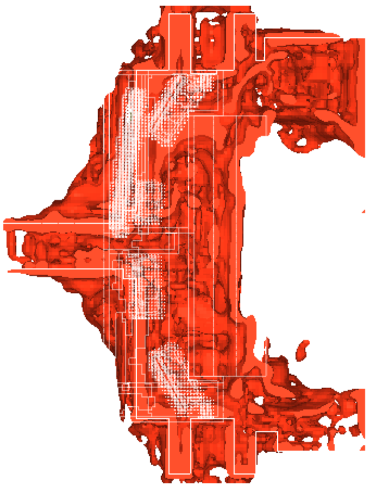

(c) Bottom view of the topology optimisation with the connection part inside.

Figure 4.2: The result of the topology optimisation.

4.4.2 Analysis of primary design

From this design, an examination of the modal analysis and strain energy was carried out on the fixture. When analysing the eigenfrequencies of the design it becomes clear that they are low compared to the BIWs. A problematic area may be the small freely hanging beam highlighted in Figure 4.3. The next part was to examine the result from strain energy to investigate if any improvements of the primary design can be done. The result of the most critical parts of the fixture regarding strain energy is on the upper parts of the A-pillar and the middle beam which can be seen in Figure 4.4.

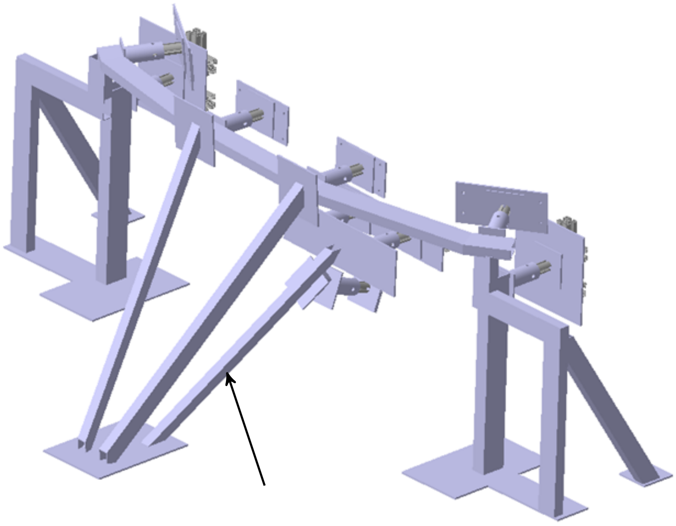

Figure 4.3: Primary design of complete generic fixture with the small beam highlighted with an arrow.

4.4.3 Final design

The final design of the generic fixture is shown in Figure 4.5. Three additional beams are added based on the result from the modal analysis and strain energy calculations on the primary fixture. The added beams are highlighted in Figure 4.5 (b) and 4.5 (c). It can be seen that one small beam is added to connect the freely hanging beam to the larger beam. It can also be seen that two larger beams are added between the rear plate and the A-pillars to stabilise the fixture furthermore. The final fixture weighs 68.8 kg which gives a 1.2 kg margin for screws and bolts and is also lower than the maximum weight constraint set on the fixture. The manufacturing of the fixture should be rather easy since the cross sections of the steel beams, steel plates, and the aluminium Aluflex$^{\text{TM}}$ profiles are broadly used in today's workshops.

4.4.4 Adjustable mechanism

Since the objective is to also make the design of the fixture generic for the two models A and B, and future models an adjustable mechanism is created. The mechanism aims to replace the main connection parts and make them adjustable in the local x, y, and z-direction. For the A-pillar brackets, for instance, see Figure 4.6, the cylinder gives flexibility in the x-direction, while the two Aluflex$^{\text{TM}}$ components that are skewed on the plate, makes for a sliding mechanism in the y-direction. Lastly, the Aluflex$^{\text{TM}}$ component that is connected to the two Aluflex$^{\text{TM}}$, gives flexibility in z-direction because of the slot. By having a generic bracket that fits both model A and B, the design of the generic bracket makes it easy to mount different models of IPs.

The centre connections between the fixture and the BIWs are made in a similar

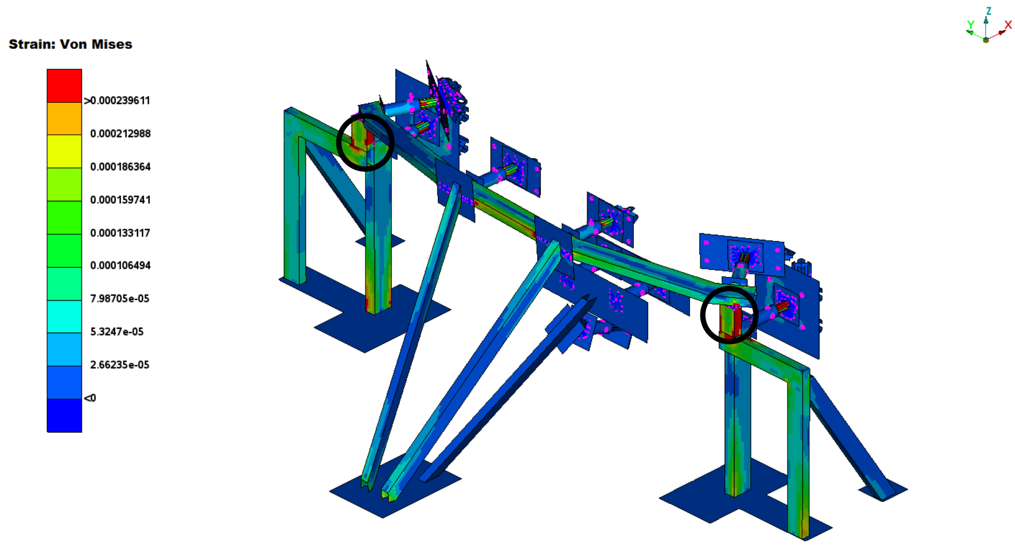

(a) The strain energy of the primary fixture with highlighted critical section.

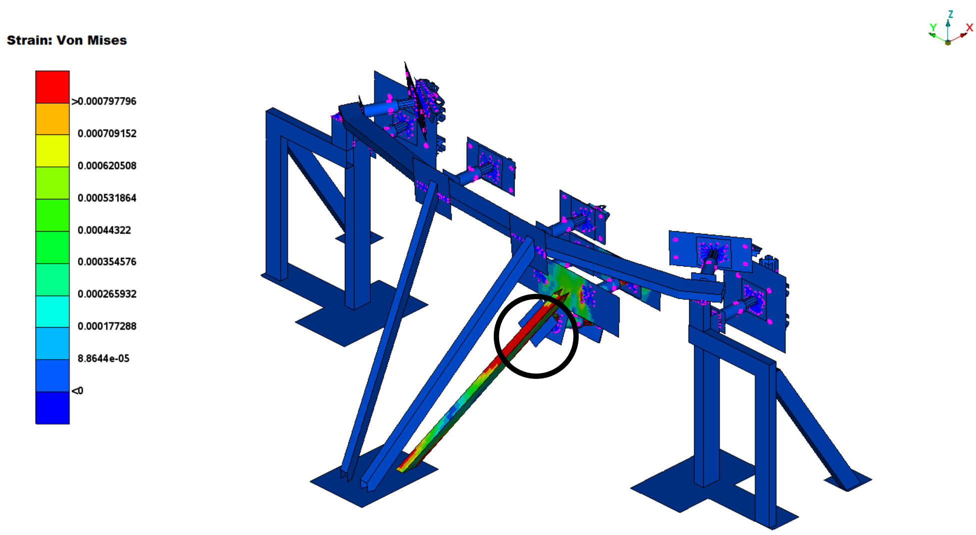

(b) The strain energy of the primary fixture with highlighted critical section.

Figure 4.4: The strain strain energy plotted on the primary fixture design.

way as for the A-pillar brackets. As seen in Figure 4.7 the cylinder gives flexibility in the x-direction, while the Aluflex$^{\text{TM}}$ component that is skewed on the plate, makes for a sliding mechanism in y-direction due to the slots.

The clips can broadly differ in geometry depending on the BIW, it was therefore decided not to replace them. Instead, the clips are welded to a plate respectively where the plate is screwed on to another plate connected to the fixture, which can be seen in Figure 4.8. The clips can thereby easily be replaced by welding different clips to a plate and screw it to the fixture plate. The adjustable mechanism used for other connections is again used here since the clips differs in the position in x-direction for the two studied BIWs.

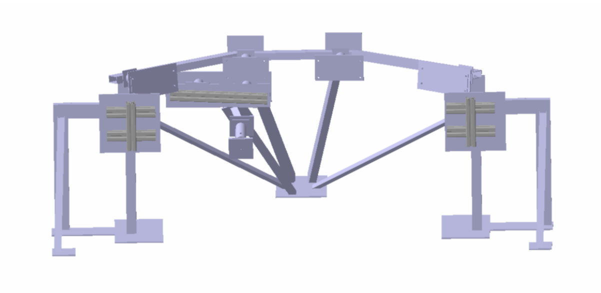

(a) Front view of the fixture design.

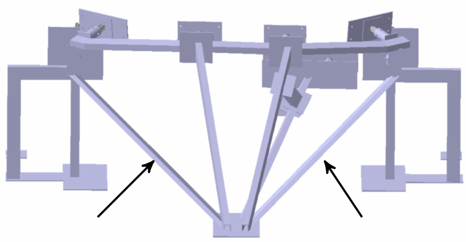

(b) Back view of the fixture with the added two beams highlighted.

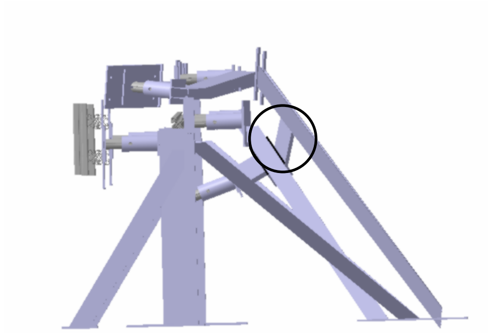

(c) Side view of the fixture with the added small beam highlighted.

Figure 4.5: The final fixture with the three added beams highlighted.

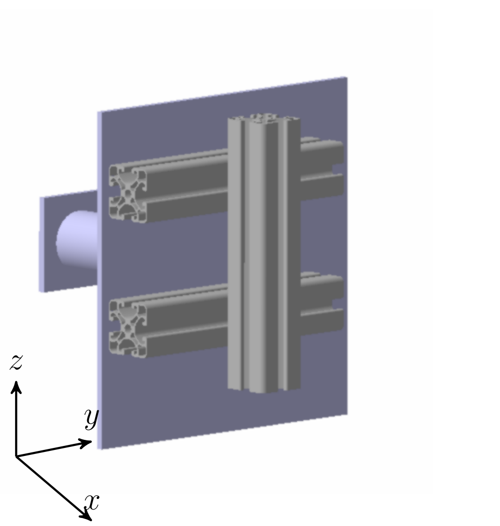

(a) Front view of the adjustable mechanism.

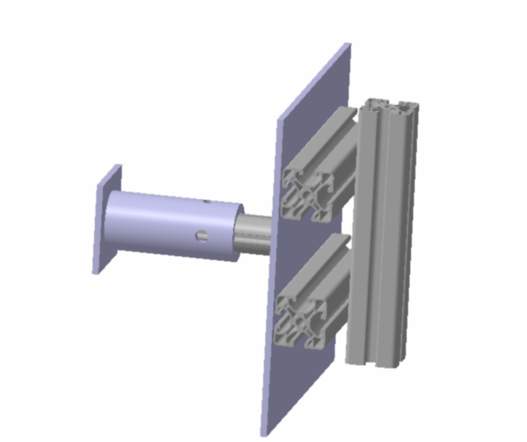

(b) Side view of the adjustable mechanism.

Figure 4.6: The adjustable mechanism of the fixture for the A-pillar brackets.

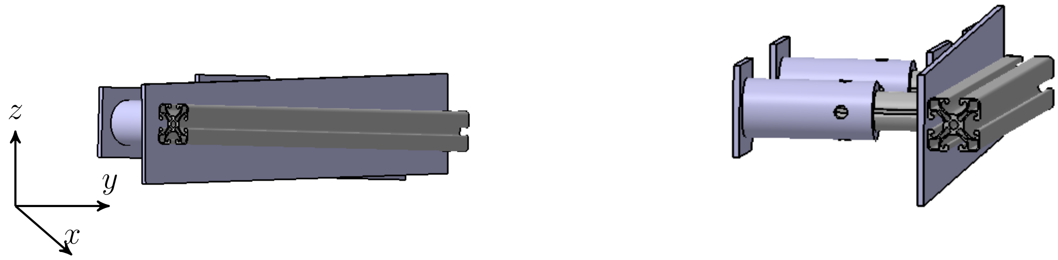

(a) Front view of the adjustable mechanism. (b) Side view of the adjustable mechanism.

Figure 4.7: The adjustable mechanism of the fixture for the centre connections.

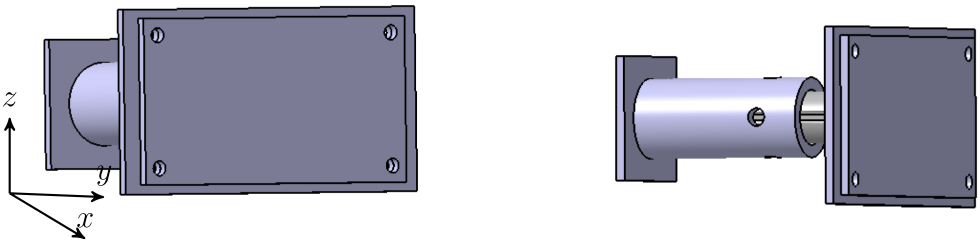

(a) Front view of the adjustable mechanism. (b) Side view of the adjustable mechanism.

Figure 4.8: Front view of the adjustable mechanism of the fixture for the clips.

4.5 Verification

The verification of the final fixture is made by mainly comparing the global and local static and dynamic stiffness of the fixture with the BIWs. Also, the modal analysis of the final fixture is performed.

4.5.1 Static stiffness

The local static stiffness is calculated in the same connection points as in the benchmark study. The difference can be seen in Figure 4.9. One reasonable explanation for this large difference in local stiffness is the aluminium material and the generic features which makes the fixture flexible in the connection points.

4.5.2 Global static stiffness

The global static stiffness of model A, B and the designed fixture are presented in Figure 4.10. It can be seen that the static stiffness in the x-direction is close to the static stiffness of the BIWs. However, when comparing the static stiffness in y and z directions it becomes clear that the fixture has significantly higher stiffness.

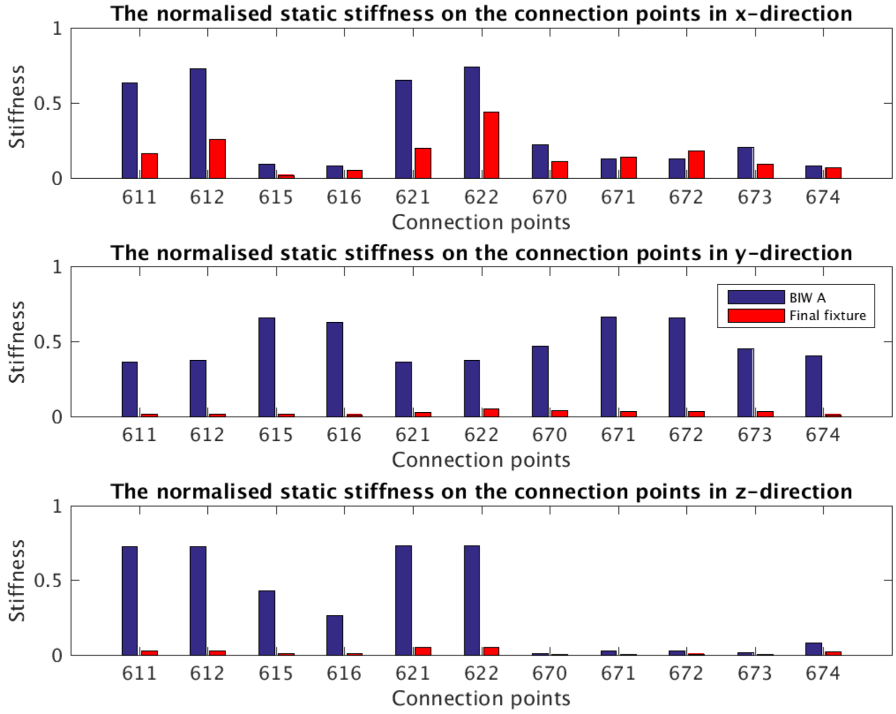

Figure 4.9: The normalised static stiffness in the connection points for model A and the final fixture.

4.5.3 Dynamic stiffness

The dynamic stiffness was computed for the fixture and the BIW of model A for the main connection points. The results can be seen in Appendix C. The graphs shows that for frequencies higher than 50 Hz the fixture has higher stiffness. For frequencies lower than 50 Hz the stiffness in the fixture is sometimes above and sometimes below of the BIW.

4.5.4 Global dynamic stiffness

The global dynamic stiffness of the BIWs and the final fixture is shown in Figure 4.11, where global dynamic stiffness of the BIWs are in the range from 1 to 50 kN/mm for all frequencies while dynamic stiffness for the fixture is much higher. Also, the dynamic stiffness in x and z-direction of the fixture has a dip at the frequencies 20 Hz and 50 Hz. This is an indication that there might be a resonance phenomenon occurring at those frequencies.

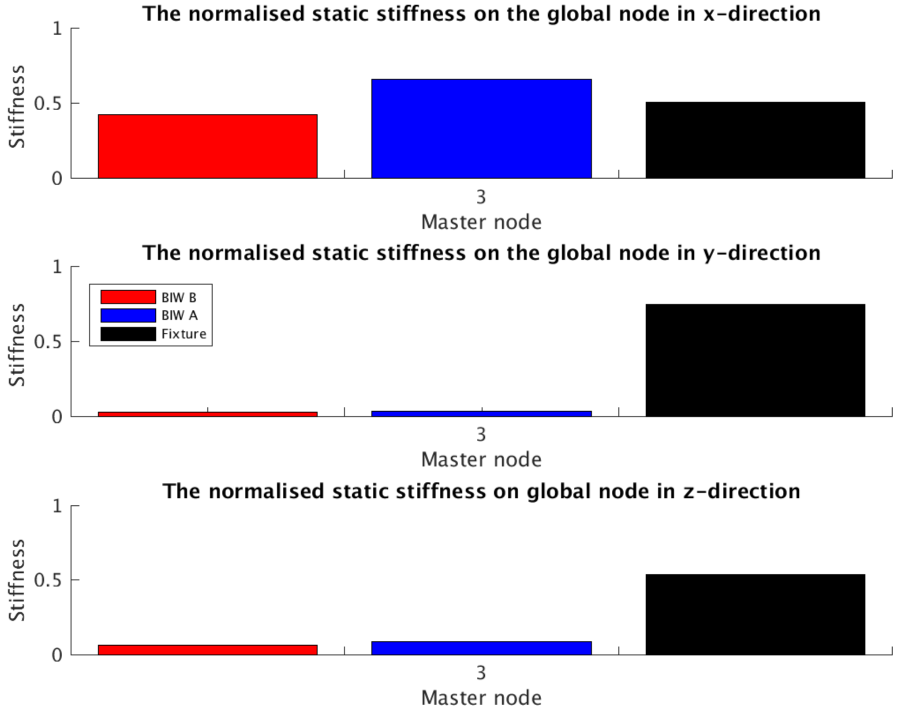

Figure 4.10: The normalised static stiffness in the global node for model A and the final fixture.

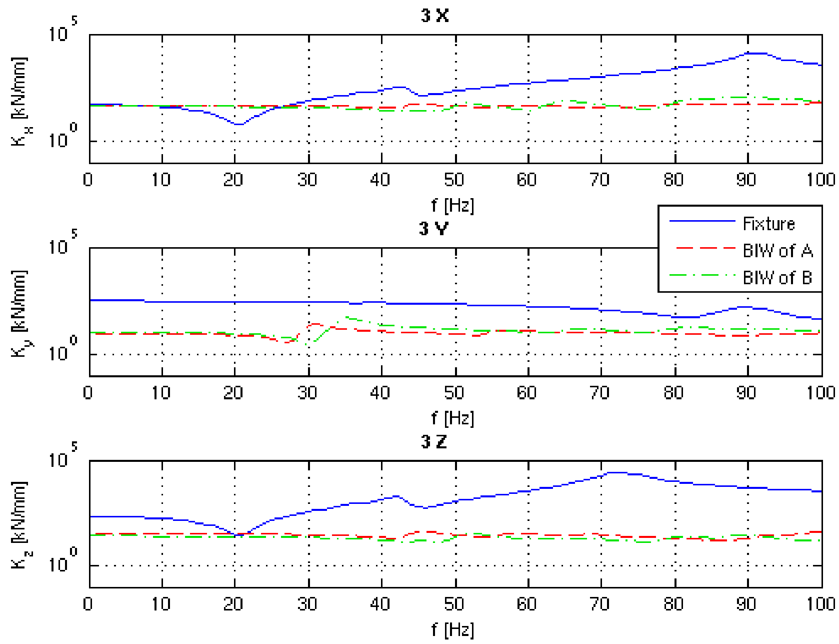

Figure 4.11: The global dynamic stiffness for the fixture compared with model A and B.

4.5.5 Modal analysis

When examining the eigenmodes of the final fixture it becomes clear why the local static stiffness is so low in comparison to the BIWs. The features which makes the fixture generic contribute to that, see Figure 4.12. Since the generic mechanism consist of an arm extension, a heavy weight is put on the extension mechanism. This is because the extension arm consist of Aluflex™, which is made of aluminium and has lower stiffness compared to steel.

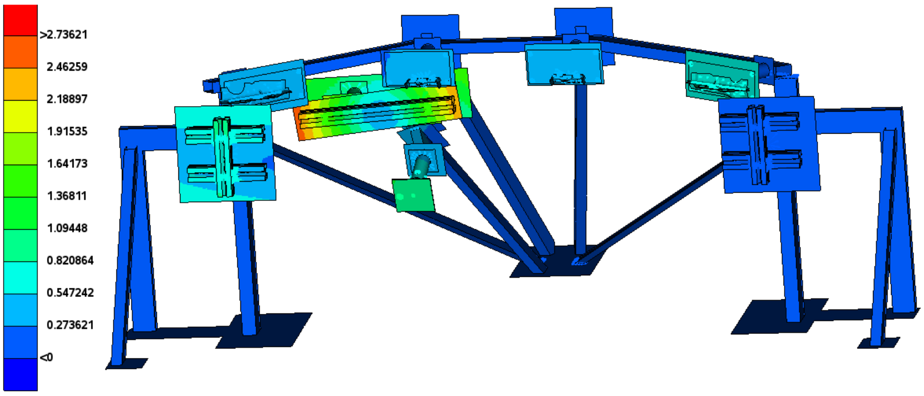

Figure 4.12: The modal behaviour of the final fixture.

5
Conclusion

5.1 Main outcome

The stated aim in section 1.2 have partly been achieved. A design of a fixture have been made, with generic features that can be manually adjusted locally. With exception for the static global stiffness in x-direction, the fixture have a higher global static and dynamic stiffness compared to the BIWs. The fixture is also manufacturable since only simple and existing geometries and cross sections were used for the design. However, the static stiffness in the local connection points where lower in the fixture compared to the BIWs.

To create a generic fixture with adjustable mechanisms has proven to be very challenging. Some design compromises for the fixture need to be made, because when having adjustable part in the design, the local stiffness of the fixture is hard maintain. The final fixture has lower stiffness in the connection points compared to the BIWs, which is not desirable. This is due to the fixture being more flexible at the adjusting mechanisms. Since the generic mechanism consist of an arm extension with Aluflex™ profile, a heavy weight is put on the extension mechanism, thus giving less local stiffness. The choice of material or the amount of material in the extension arm may be important factors for obtaining a stiffer structure locally. A conclusion of this is that adjustable parts make the structure less rigid, which results in low local stiffness values.

5.2 Future recommendations

A further investigation into how to stiffen up the local stiffness of the adjustable mechanism is recommended. The local stiffness of the fixture can be increased by adding additional beams in a triangle design, since a triangular structure results in a more rigid structure. Another alternative to increase the local stiffness of the fixture is to replace the beam structure with a frame structure. This frame structure can be imagined from the not-so-easy-to-interpret results from the topology optimisation. The weight limitation for the fixture can however be an obstacle for a frame structure design.

It was shown that the aluminium profiles might not be the best choice for this design of the adjustable mechanisms. The aluminium structure have lower stiffness as compared to steel. Steel is probably the best choice of material for the fixture due to its higher rigidity. However, the structures of the aluminium Aluflex™ profiles are very complex and it would be both difficult and expensive to manufacture them in steel. Steel is also very heavy and there is a restriction on how much weight the shaker rig can excite.

Another option, is to do a more intensely study for a global and local adjustable stiffness mechanism, since very few stiffness adjustable mechanisms were found in the searches made in this thesis work. Those that were found, were only prototypes and were rejected for this project because of their size.

Bibliography

[1] M.Trapp, F.Chen. *Automotive Buzz, Squeak and Rattle: Mechanisms, Analysis, Evaluation and Prevention.* Oxford, Butterworth-Heinemann, 2012.

[2] F.Kavarana, B.Rediers. *Squeak and Rattle – State of the Art and Beyond.* Michigan, 2001.

[3] Toolsqa. *Difference between Verification and Validation*, 2017.
URL: https://www.toolsqa.com/software-testing/difference-between-verification-and-validation/

[4] Wikipedia contributors. *Modal analysis.*
Wikipedia, The Free Encyclopedia, 2019,
URL: https://en.wikipedia.org/wiki/Modal_analysis

[5] P.Guillaume *Modal Analysis.* Vrije Universiteit Brussel, 2007.
URL: http://mech.vub.ac.be/avrg/publications/ModalAnalysis.pdf

[6] R.R.Crag, A.Kurdila. *Fundamentals of structural Dynamics, 2nd edn.* John Wiley & Sons Inc, 2006.

[7] P.Baumgart. *Stiffness- an unknown world of mechanical science?.* Elsevier Ltd, 2000.

[8] T.Abrahamsson. *Calibration and Validation of Structural Dynamics Models.* Chalmers University of Technology, 2012.

[9] Allan G.Piersol, Thomas L.Paez. *Harris' shock and vibration handbook, 6th edition.* McGraw-Hill, 2010.

[10] B.Rediers, B.Yang, V.Juneja. *Static and Dynamic stiffness: One test, both results.*
URL: https://pdfs.semanticscholar.org/d23d/29bf2883883fa49859f0bb53ce33ca3ccaec.pdf

[11] Wikipedia contributors. *Topology optimization.* The Free Encyclopedia, 2019
URL: https://en.wikipedia.org/wiki/Topology_optimization

[12] M.Zhou, R.Fleury, Y.K.Shyy, H.Thomas, J.M.Brennan. *Progress in Topology Optimization with Manufacturing Constraints.* Altair Engineering Inc, 2002.

[13] HyperWorks Solvers. *Gradient-based Optimization Method.*
URL: https://cdm.ing.unimo.it/files/master/Veicolo_2018/Body_in_white/Lesson_optimization/Gradient_based_optimization_method.pdf

A

Appendix 1

A.1 Dynamic stiffness

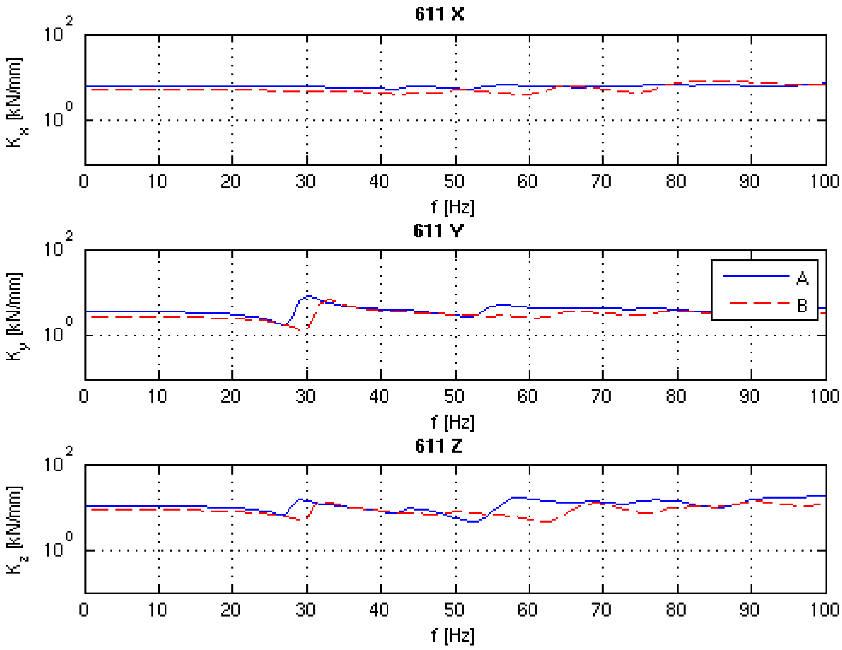

Figure A.1: Dynamic stiffness in x, y and z-direction for the connection point 611 for models A and B.

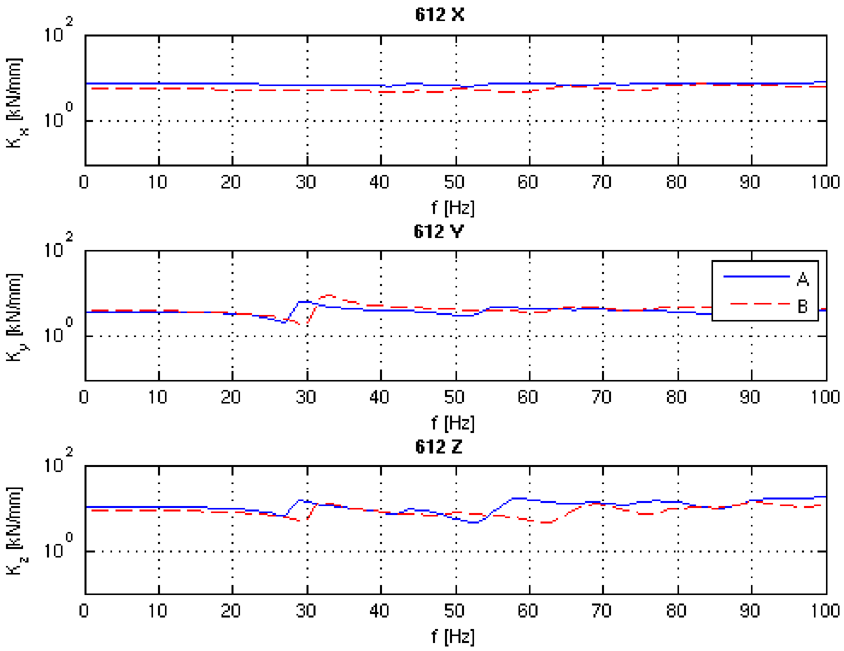

Figure A.2: Dynamic stiffness in x, y and z-direction for the connection point 612 for models A and B.

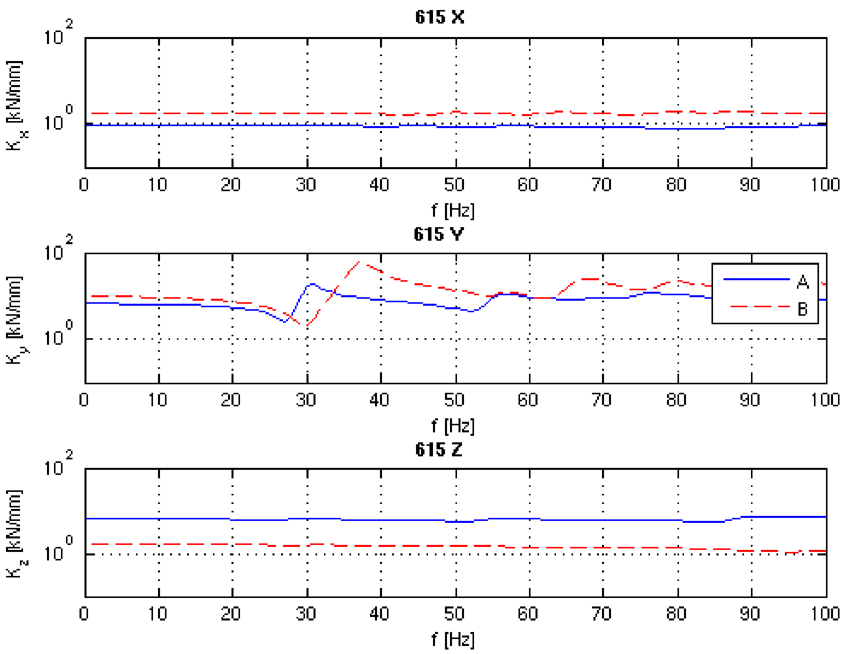

Figure A.3: Dynamic stiffness in x, y and z-direction for the connection point 615 for models A and B.

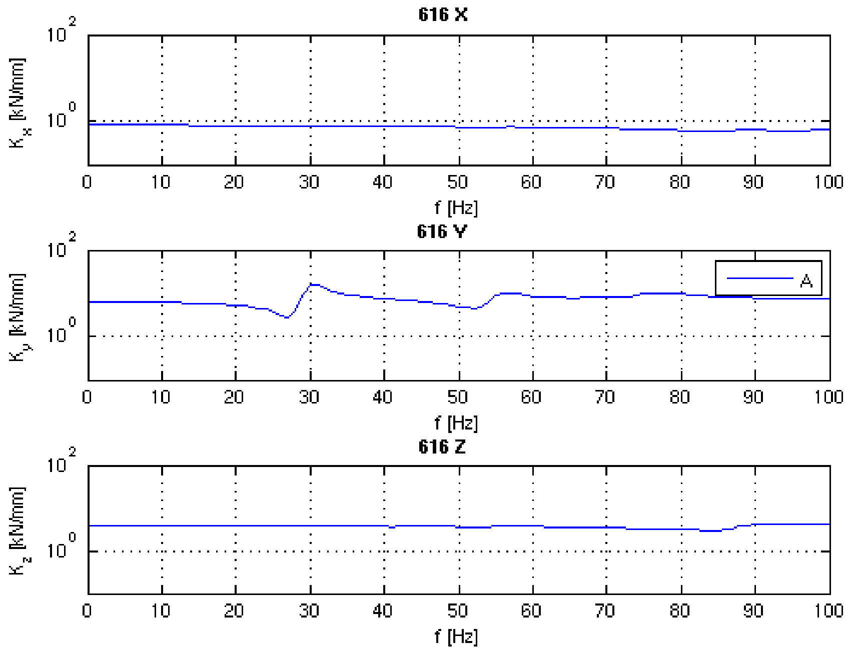

Figure A.4: Dynamic stiffness in x, y and z-direction for the connection point 616 for models A and B.

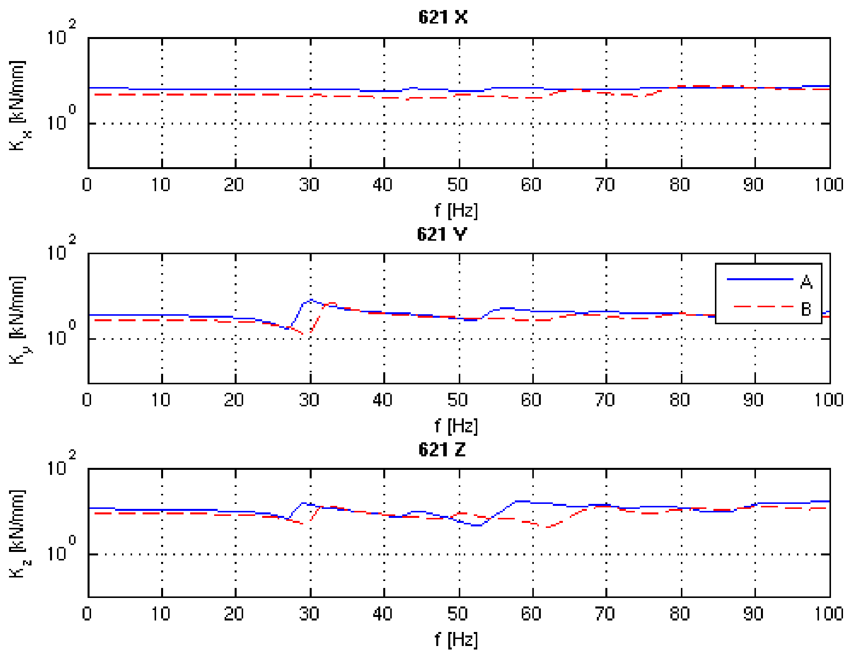

Figure A.5: Dynamic stiffness in x, y and z-direction for the connection point 621 for models A and B.

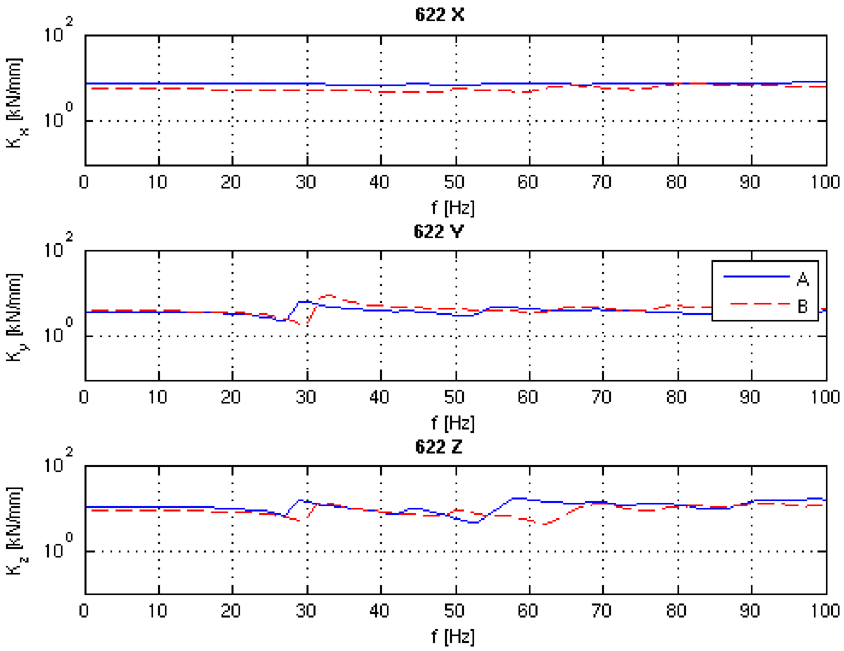

Figure A.6: Dynamic stiffness in x, y and z-direction for the connection point 622 for models A and B.

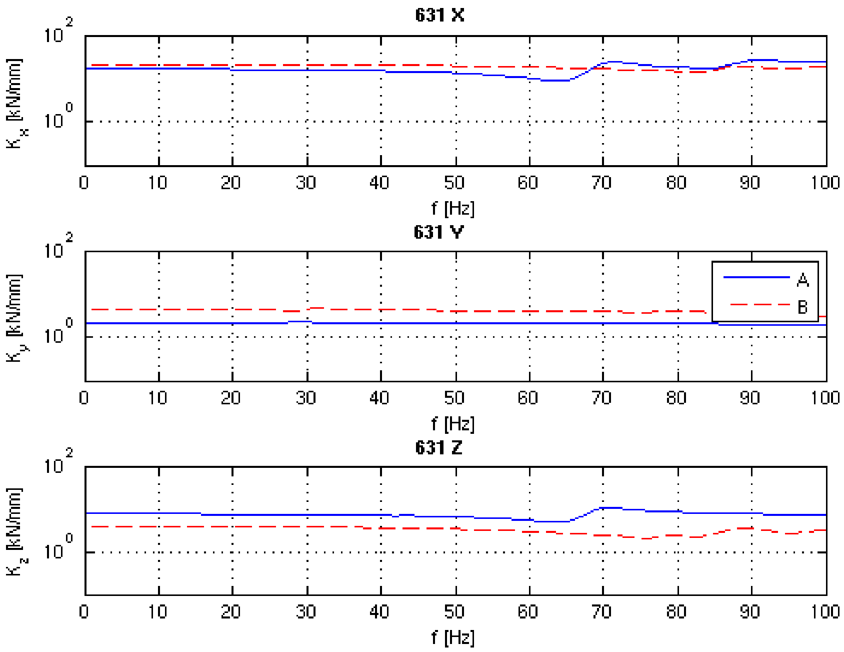

Figure A.7: Dynamic stiffness in x, y and z-direction for the connection point 631 for models A and B.

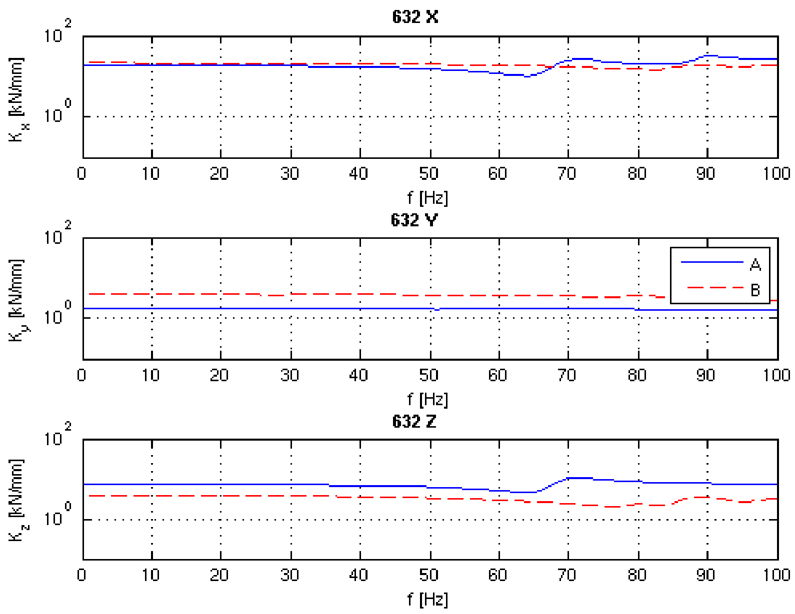

Figure A.8: Dynamic stiffness in x, y and z-direction for the connection point 632 for models A and B.

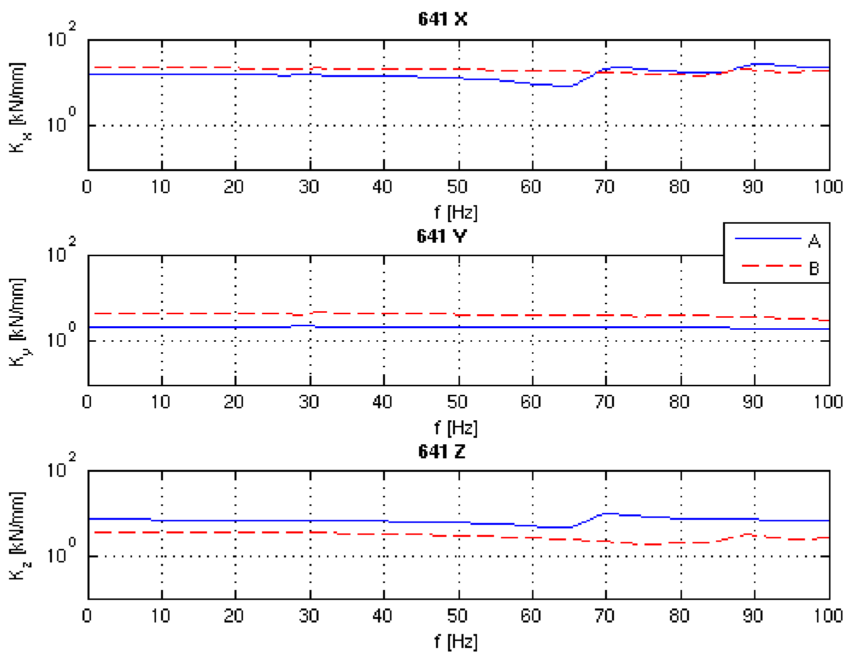

Figure A.9: Dynamic stiffness in x, y and z-direction for the connection point 641 for models A and B.

B

Appendix 1

B.1 Sine Sweep Signals

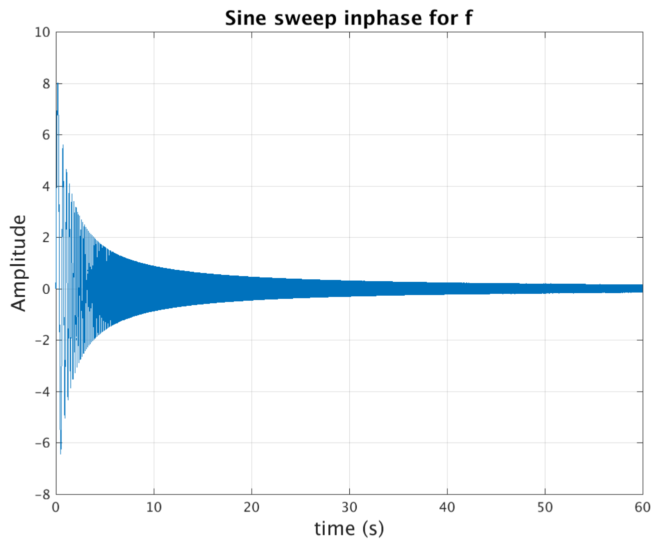

(a) In-phase sine sweep signal in time domain for $A = \frac{A_0}{f}$.

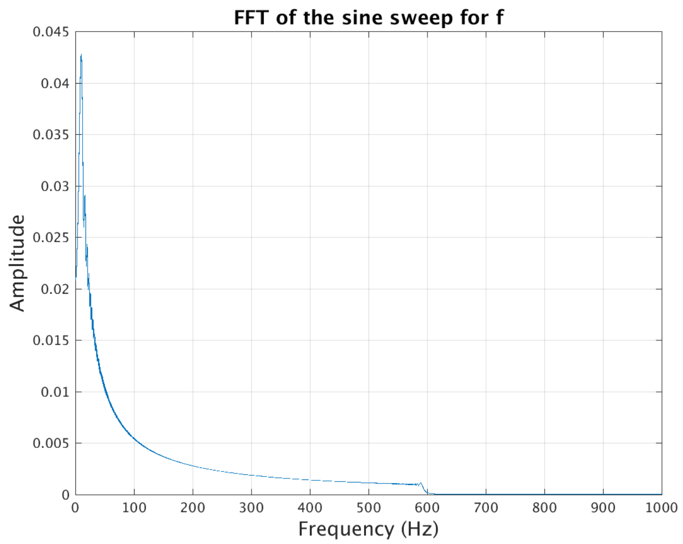

(b) FFT of the in-phase sine sweep signal for $A = \frac{A_0}{f}$.

Figure B.1: In-phase sine sweep signal for the case $A = \frac{A_0}{f}$.

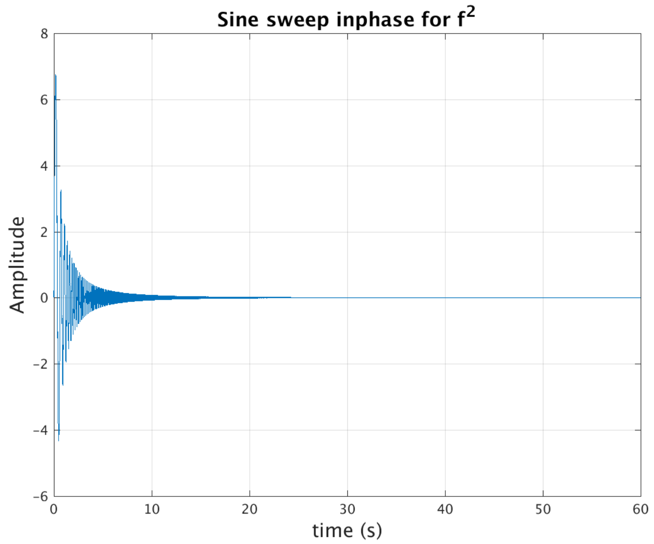

(a) In-phase sine sweep signal in time domain for $A = \frac{A_0}{f^2}$.

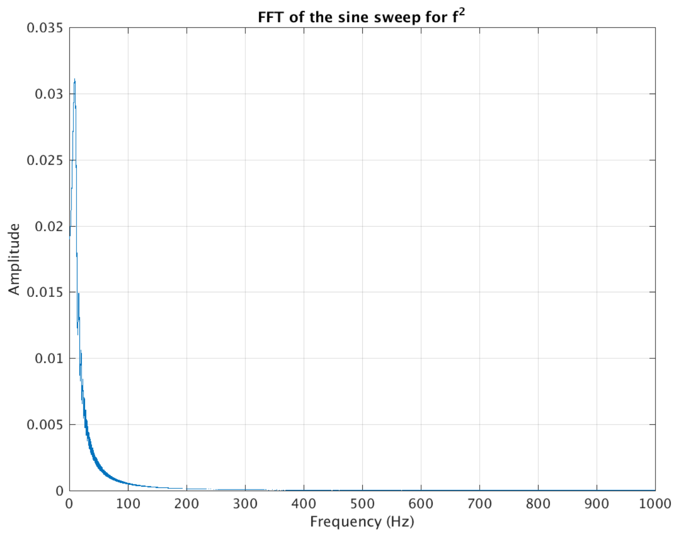

(b) FFT of the in-phase sine sweep signal for $A = \frac{A_0}{f^2}$.

Figure B.2: In-phase sine sweep signal for the case $A = \frac{A_0}{f^2}$.

B.2 Quality Check

B.2.1 Model A

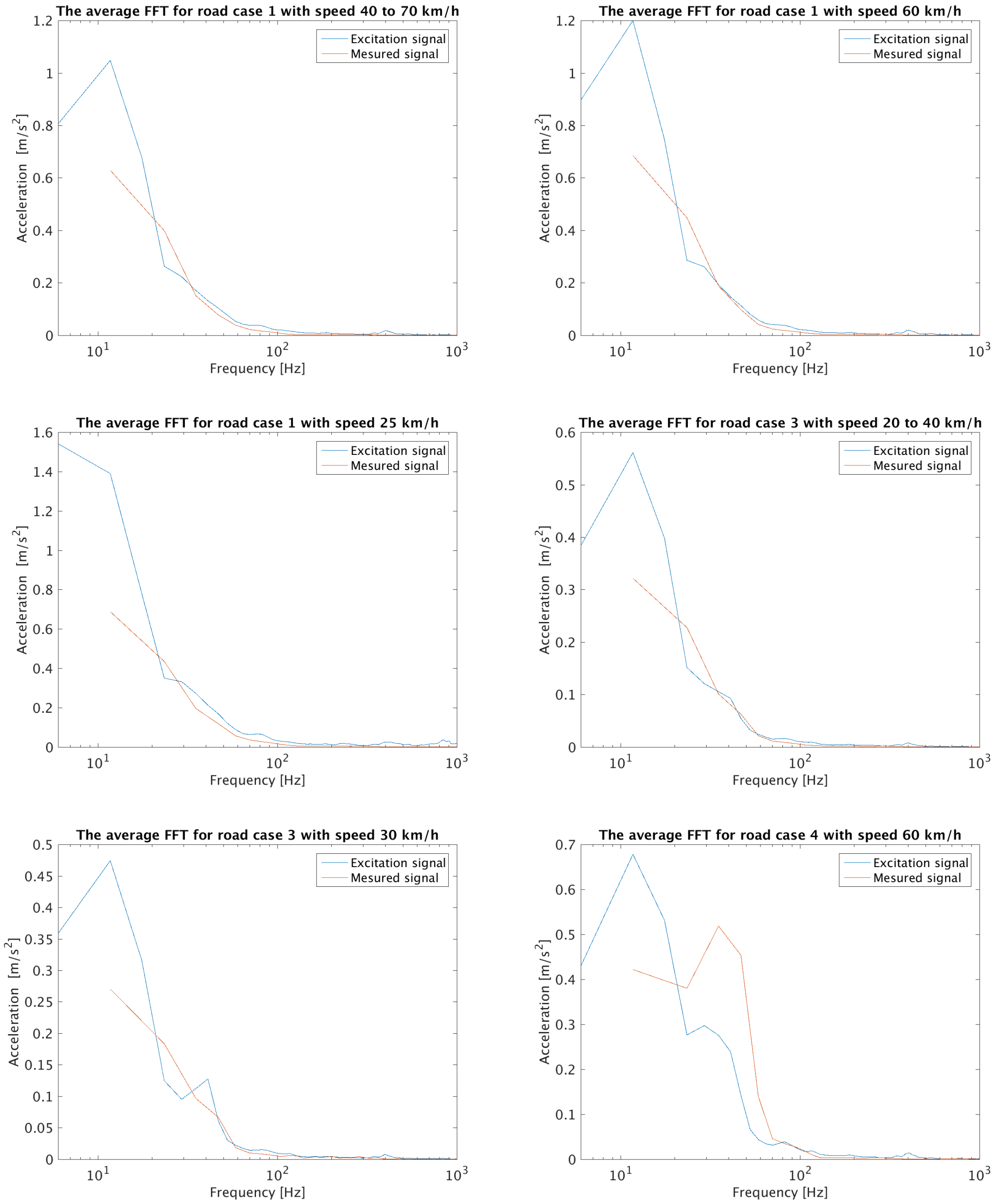

Figure B.3: Quality check of the measured signals compared to the excited signals for the model A.

B.2.2 Model B

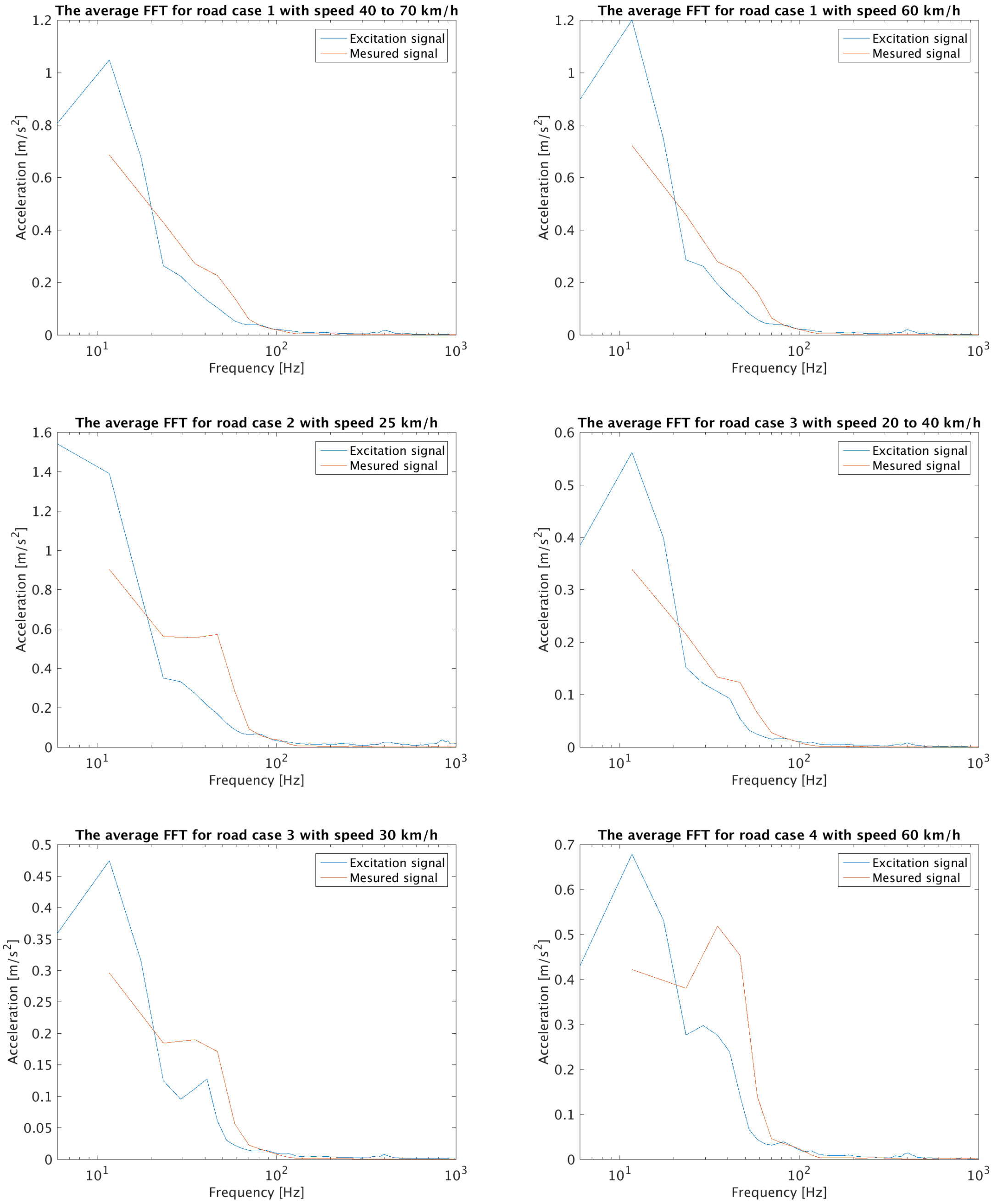

Figure B.4: Quality check of the measured signals compared to the excited signals for the model B.

C

Appendix 2

C.1 Dynamic stiffness: Fixture vs BIW

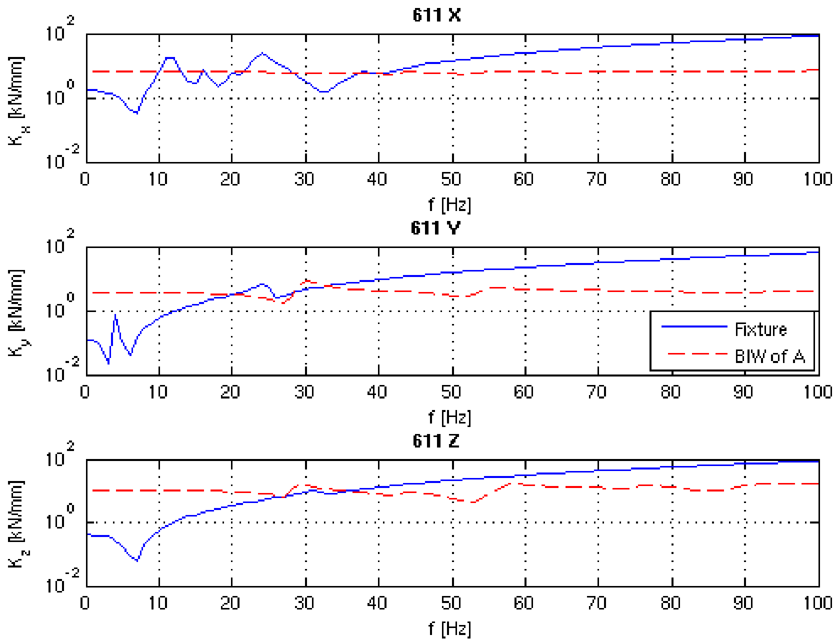

Figure C.1: The dynamic stiffness for node 611 in the main connection points for the BIW of model A compared with the fixture.

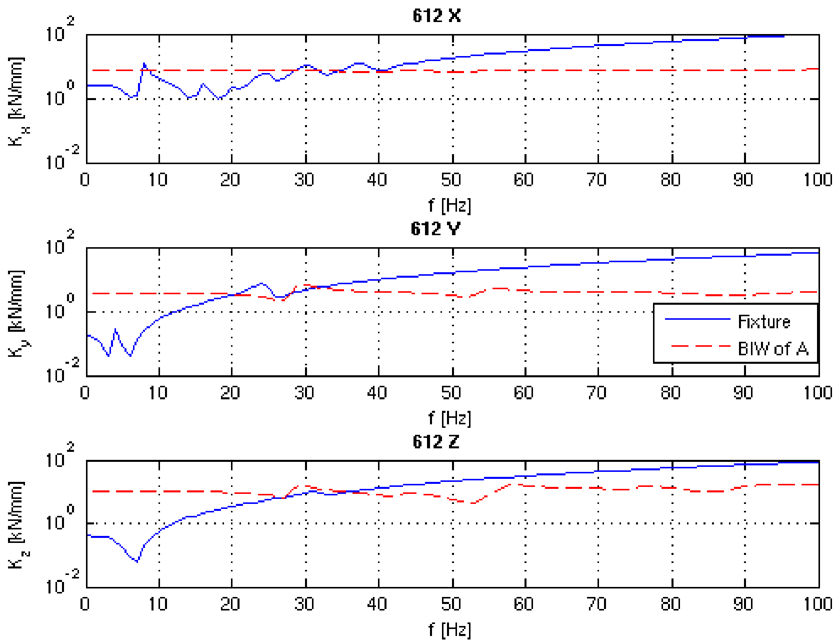

Figure C.2: The dynamic stiffness for node 612 in the main connection points for the BIW of model A compared with the fixture.

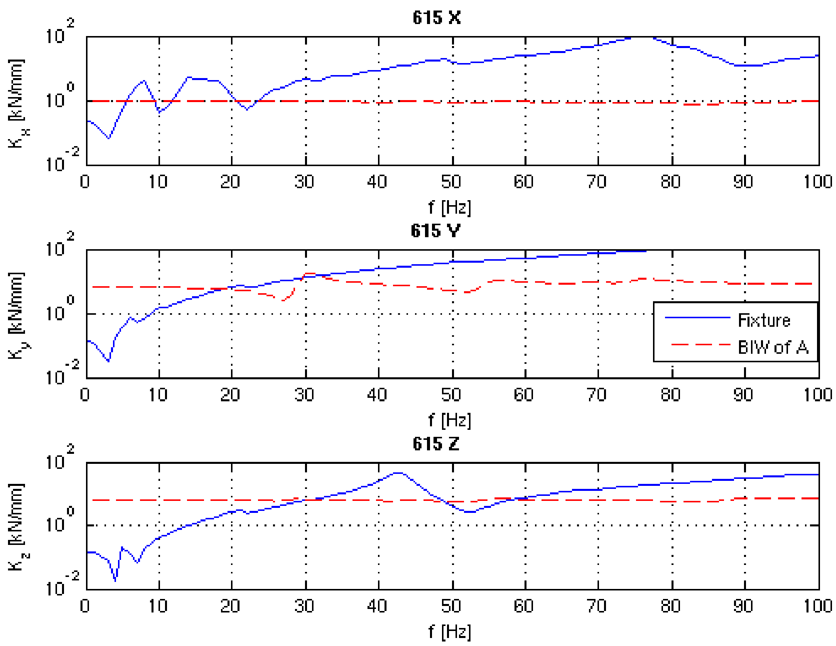

Figure C.3: The dynamic stiffness for node 615 in the main connection points for the BIW of model A compared with the fixture.

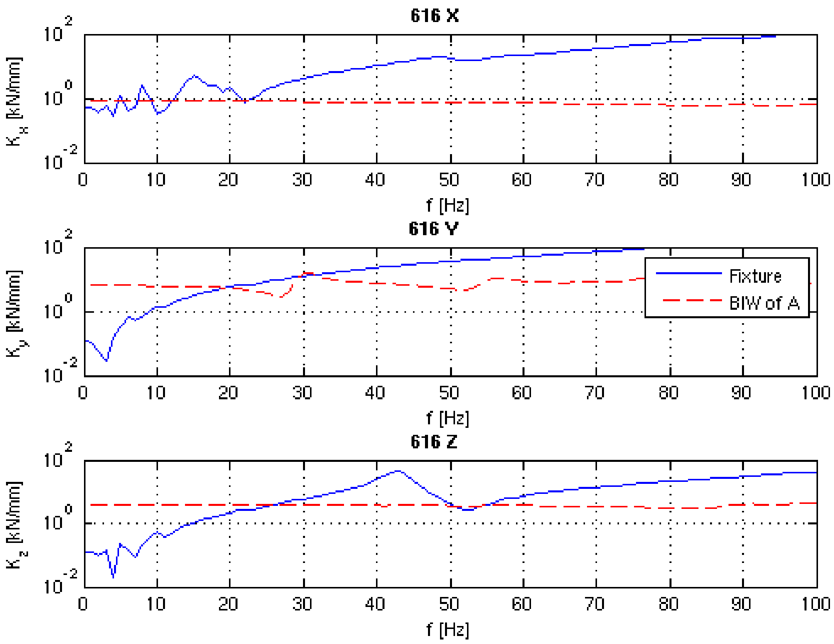

Figure C.4: The dynamic stiffness for node 616 in the main connection points for the BIW of model A compared with the fixture.

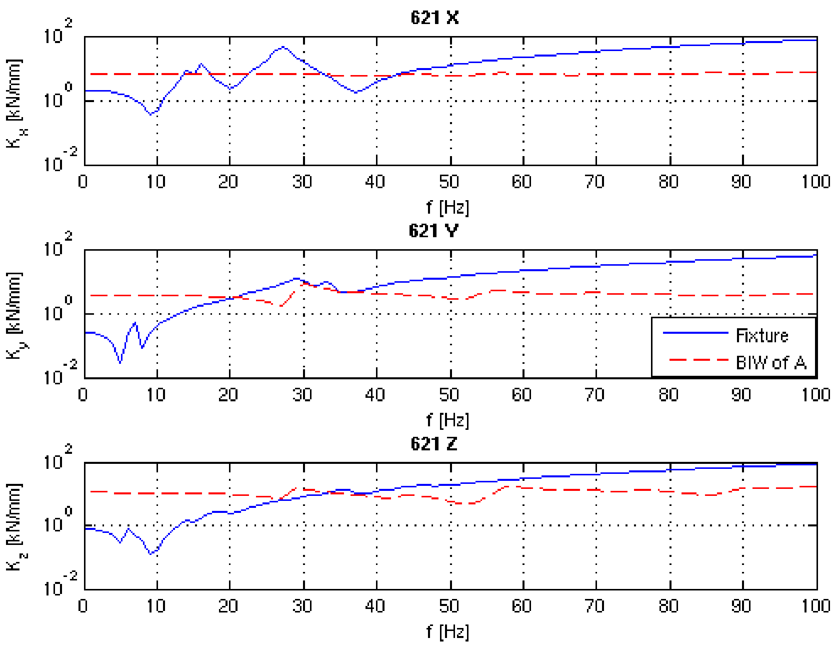

Figure C.5: The dynamic stiffness for node 621 in the main connection points for the BIW of model A compared with the fixture.

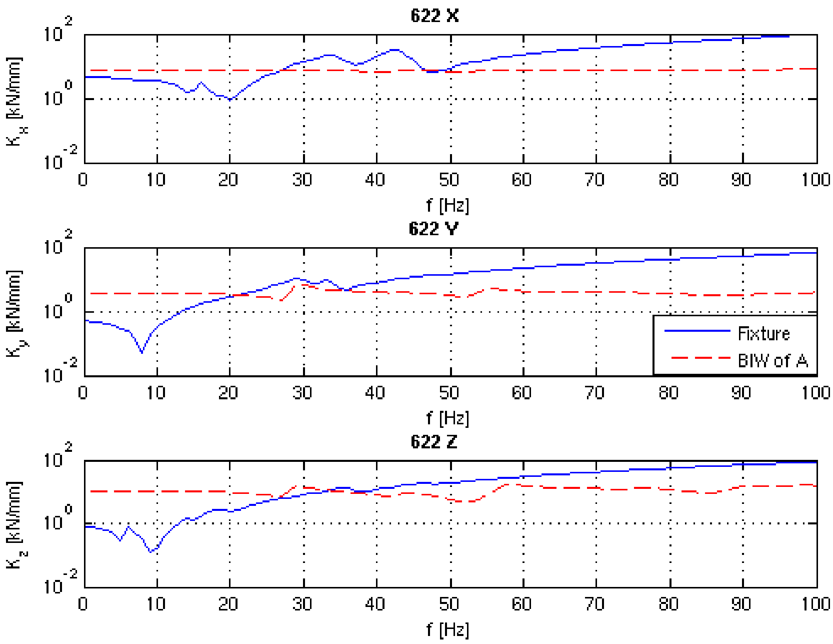

Figure C.6: The dynamic stiffness for node 622 in the main connection points for the BIW of model A compared with the fixture.